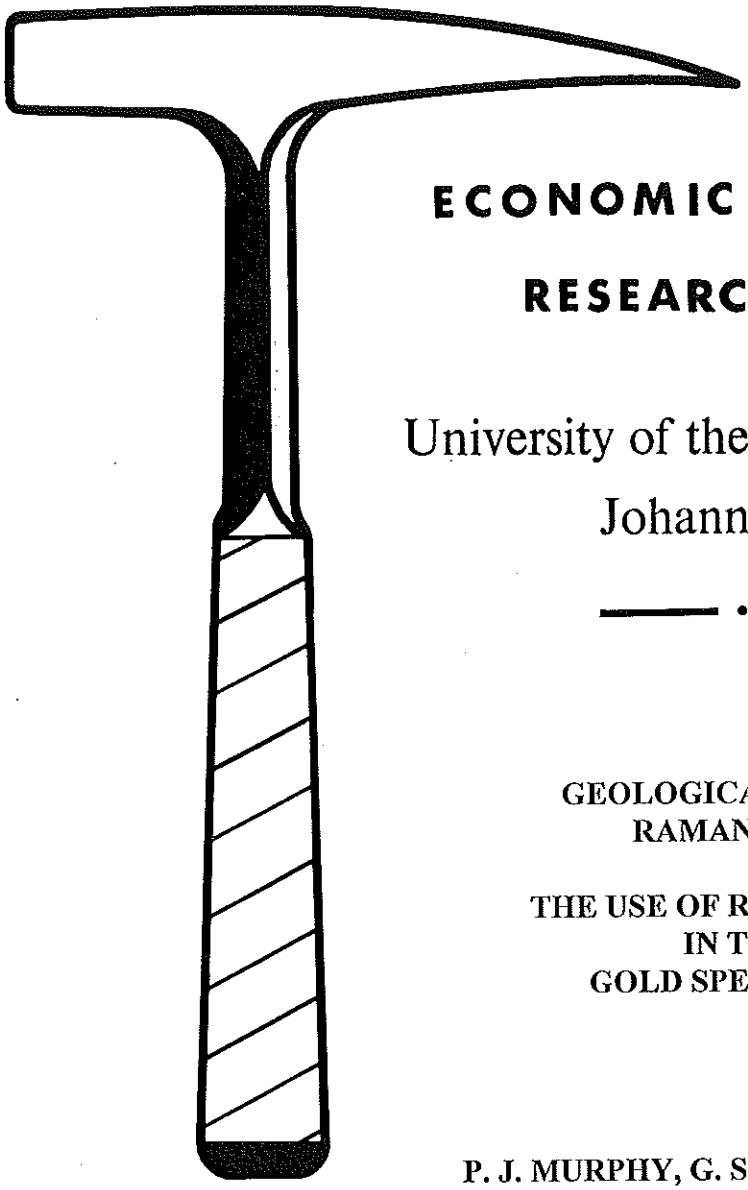

ECONOMIC GEOLOGY

RESEARCH UNIT

University of the Witwatersrand

Johannesburg

GEOLOGICAL APPLICATIONS OF RAMAN SPECTROSCOPY AND THE USE OF RAMAN SPECTROSCOPY IN THE STUDY OF GOLD SPECIATION IN FLUIDS

P. J. MURPHY, G. STEVENS and M. S. LAGRANGE

INFORMATION CIRCULAR No. 321

UNIVERSITY OF THE WITWATERSRAND
JOHANNESBURG

GEOLOGICAL APPLICATIONS OF RAMAN SPECTROSCOPY AND THE USE OF RAMAN SPECTROSCOPY IN THE STUDY OF GOLD SPECIATION IN FLUIDS

by

P.J. MURPHY [1,2]

With contributions by

G. STEVENS [2] and **M.S. LAGRANGE*** [2]

1: Raman and Luminescence Laboratory, Department of Physics
2: Economic Geology Research Unit, University of the Witwatersrand, Private Bag 3, WITS 2050, South Africa

* Present Address: Department of Geology, University of Cape Town

ECONOMIC GEOLOGY RESEARCH UNIT
INFORMATION CIRCULAR No. 321

April,1998

GEOLOGICAL APPLICATIONS OF RAMAN SPECTROSCOPY AND THE USE OF RAMAN SPECTROSCOPY IN THE STUDY OF GOLD SPECIATION IN FLUIDS

ABSTRACT

Raman Spectroscopy is a method of measuring vibrational frequencies of molecules and the lattice vibrations of crystalline materials. As such, it studies the structure, rather than the chemical composition, of a sample, although the composition can often be inferred. The technique is very flexible, and can be applied to samples in liquid, solution or solid form. It can be used via a microscope, allowing *in situ* analysis of thin or polished sections, and, with suitable equipment, at a range of temperatures and pressures.

The technique has a wide range of applications in the Earth Sciences, including: characterisation of minerals, including distinguishing between polymorphs or identifying microscopic inclusions; study of the products of sulphide oxidation or mineral processing reactions; analysis of gases or hydrocarbons in fluid inclusions; monitoring of structural changes in minerals with applied temperature or pressure; monitoring of strain in crystals; and the study of metal speciation in natural or hydrothermal fluids.

The latter application is used in this circular as an extended example of the application of Raman spectroscopy to geological problems. Raman analysis is an ideal method for studying hydrothermal fluids as it allows direct observation of the solution at hydrothermal conditions, and the technique allows interpretation of the structure of the metal complexes present. In this case the system studied was the gold-chloride-hydroxide system, at ambient temperature and pressure, and varying pH and chloride concentration. Previous work on gold chloride speciation in fluids has shown differences in opinion as to the relative importance of gold (I) and gold (III) species, as well as for the Raman peak assignments for the various species. In addition, previous experimental work is not consistent with theoretical predictions either of the number or of the frequencies of the peaks in the Raman spectrum.

In order to re-evaluate the effect of pH on Raman spectra and speciation, solutions containing gold (III) chloride were analysed by Raman spectroscopy at ambient temperature and pressure, over a range of pH from 1 to 11. Total gold concentrations were from 0.02 to 0.001M, with total chloride concentrations of 0.004-0.1M. The spectra obtained are consistent with the hydrolysis sequence of square-planar Au(III) complex ions $[AuCl_x(OH)_{4-x}]^-$, where x = 0 to 4. $[Au(OH)_4]^-$ probably occurred, alongside $[AuCl(OH)_3]^-$ at pH values above 11. A dark purplish-grey precipitate (Au(I)OH) formed at high pH values. No evidence for Au(I) species was found.

The spectra are more consistent with theory than previous data, and show the predicted number of peaks for Au-Cl and Au-OH stretches for each species. However, the peak frequencies do not fit precisely with the predictions of Tossell (1996), particularly for Au-OH stretches. Significant differences were found between the pH values of hydrolysis and those presented in previous works, and both gold and chloride concentration were found to affect the pH ranges of stability for the various chloro-hydroxy species.

A hydrothermal cell has been developed which allows Raman analysis of fluids at hydrothermal conditions, up to 350°C and 2kbar and in future this will be used to extend this study to conditions relevant to the formation of many lode gold deposits.

oOo

GEOLOGICAL APPLICATIONS OF RAMAN SPECTROSCOPY AND THE USE OF RAMAN SPECTROSCOPY IN THE STUDY OF GOLD SPECIATION IN FLUIDS

CONTENTS

_____oOo _____

Published by the Economic Geology Research Unit
Department of Geology
University of the Witwatersrand
1 Jan Smuts Avenue
Johannesburg 2001
South Africa

ISBN 1-86838-208-7

GEOLOGICAL APPLICATIONS OF RAMAN SPECTROSCOPY AND THE USE OF RAMAN SPECTROSCOPY IN THE STUDY OF GOLD SPECIATION IN FLUIDS

PART ONE: AN INTRODUCTION TO RAMAN SPECTROSCOPY AND ITS GEOLOGICAL APPLICATIONS

INTRODUCTION

Raman spectroscopy is a technique that has a wide range of applications in the Earth Sciences, and the aim of this circular is to provide an overview of the technique and of applications of interest to geologists, particularly in the field of mineral deposits. This will be highlighted by an extended example of Raman analysis of gold speciation in fluids, to illustrate the type of work that is being carried out in the new Raman and Luminescence Laboratory at Wits, by members of GRU.

Like X-ray diffraction analysis, Raman spectroscopy studies the structure of a sample, but in the case of Raman analysis the molecular, rather than the crystal structure is studied. The technique can therefore be applied to different phases: gas and liquid as well as crystalline or powdered samples. It can also be used under a range of conditions of temperature or pressure. Via a microscope it can be used on a micro-scale to study samples in situ, including conventional polished or petrographic thin sections. Maps or traverses of an area can be made in order to study variations in composition or structure.

Raman Spectroscopy is essentially a method of measuring vibrational frequencies of molecules and the lattice vibrations of crystalline materials. Thus it is extremely useful in a wide range of geological applications:

- Identification of an unknown mineral sample
- Distinguishing between mineral polymorphs
- Verification of the presence of a given species in a sample
- Estimation of relative proportions of different species within a sample
- Interpretation of the structure of a sample (particularly alongside infrared absorption spectroscopy)
- Monitoring of the changes in structure with external conditions (temperature, pressure, etc.)
- Monitoring of strain in crystals

THEORY

In order to understand the range of applications, a certain amount of theory must be considered. However, this section will be kept as brief as possible and illustrated by geological examples.

The Raman Effect

When light is incident on a sample, a portion if it is absorbed and then scattered back at the same frequency. This is known as elastic, or Rayleigh scattered light, and has an intensity of $\approx 10^{-3}$ that of the incident light. A much smaller portion of the light is changed in frequency and this is known as inelastic, or Raman scattered light. The Raman effect, which is due to the interaction of

the light with molecular vibrations, was first described by Raman and Krishnan (1928). The changes in the frequency of the light are caused by molecular vibrations, both within and between molecules in the sample. The resulting spectrum therefore reflects the molecular structure and symmetry of the illuminated matter, and since lattice vibrations are sensitive to local environments, the microscopic nature of structural and/or compositional disorder can also be interpreted.

The difference in frequency between the incident and scattered light (known as the Raman shift) is both positive and negative, and follows the form:

$$\nu' = \nu_o \pm \nu_M$$

where ν_o is the incident wavenumber and ν_M lies in the range of rotational, vibrational, and electronic transitions.

When $\nu' = \nu_o - \nu_M$ the scattered light is known as Stokes radiation, while when $\nu' = \nu_o + \nu_M$ it is termed anti-Stokes. Stokes peaks are generally more intense than anti-Stokes, and are therefore more usually measured. Since the magnitude of the Raman shift is independent of the exciting frequency, the position of a peak is usually described in terms of Rcm^{-1}, that is the frequency relative to the exciting line, rather than the absolute frequency.

Except at absolute zero, all substances have a certain amount of vibrational energy, due to atoms moving relative to each other as bonds stretch, compress and bend. It is these bond vibrations that cause the shifts in energy that result in the Raman effect. Two different models are used to describe the mechanism of Raman scattering. Both produce the same results, but in certain circumstances one may allow a clearer understanding of certain phenomena than the other. However, it must be remembered that they are in effect describing the same process.

Classical model

Under the classical model individual vibrations within the molecules are considered. Electric and magnetic dipoles are induced in the scattering system by incident radiation. Not all vibrations in a molecule will produce Raman peaks. In order for a vibration to be Raman active, it must result in a change in the polarizability of the molecule. During a vibration, swelling and contraction of the molecule changes the amount of control the nuclei have over the electrons, and therefore the polarizability. In the complementary vibrational spectroscopy technique of Infrared Absorption Spectroscopy a bond vibration must result in a change in the dipole moment, for it to be infrared active. Thus a vibration may be either Raman or Infrared active, or active in both or neither.

In simple molecules, straightforward inspection allows the determination of whether or not certain bond vibrations will result in Raman peaks. However, in more complicated molecules, and particularly in crystals, the analysis becomes too complicated and mathematical methods must be employed.

Energy transfer model

The energy transfer model is essentially a quantum mechanical explanation for Raman spectra, as it assumes discrete energy levels within the molecule. Photons from a light source collide with molecules of the samples, there is an energy transfer, and new photons are emitted.

A photon, with a frequency ω_i is incident on the sample and is destroyed (Fig. 1a). A new photon, of frequency ω_s with higher or lower energy than incident light is created, along with a phonon (a quantum of vibrational energy) of frequency ω. The frequencies are related by the equation $\omega_i = \omega_s + \omega$. The frequency of the vibrational phonon is therefore reflected in the Raman shift, or the difference in the scattered light relative to the incident light (Fig. 1b). Thus

the peaks of light in a Raman spectrum reflect the frequencies of molecular vibrations within the sample.

This can be seen as a movement between energy levels (Fig.1c): the molecule moves from low energy level E_1 to upper level E_2, as it acquires energy $\Delta E=E_2-E_1$ from the incident radiation. For Rayleigh scattering, the molecule is excited to a "virtual" state of higher energy, but rapidly returns to the ground state: no change in the overall energy occurs, and so there is no change in the frequency. For Stokes scattering, an incident photon of energy is destroyed, and energy is absorbed as the molecule is excited to a higher energy state. It then returns to an energy level slightly higher than the ground state, emitting a photon at higher energy than the incident light, and there is an associated positive change in frequency of the scattered light. For antiStokes scattering, the molecule begins in a higher energy state and returns to the ground state, creating a photon of lower energy than the incident photon. This effect is generally weaker, as fewer systems will initially be in the higher energy state.

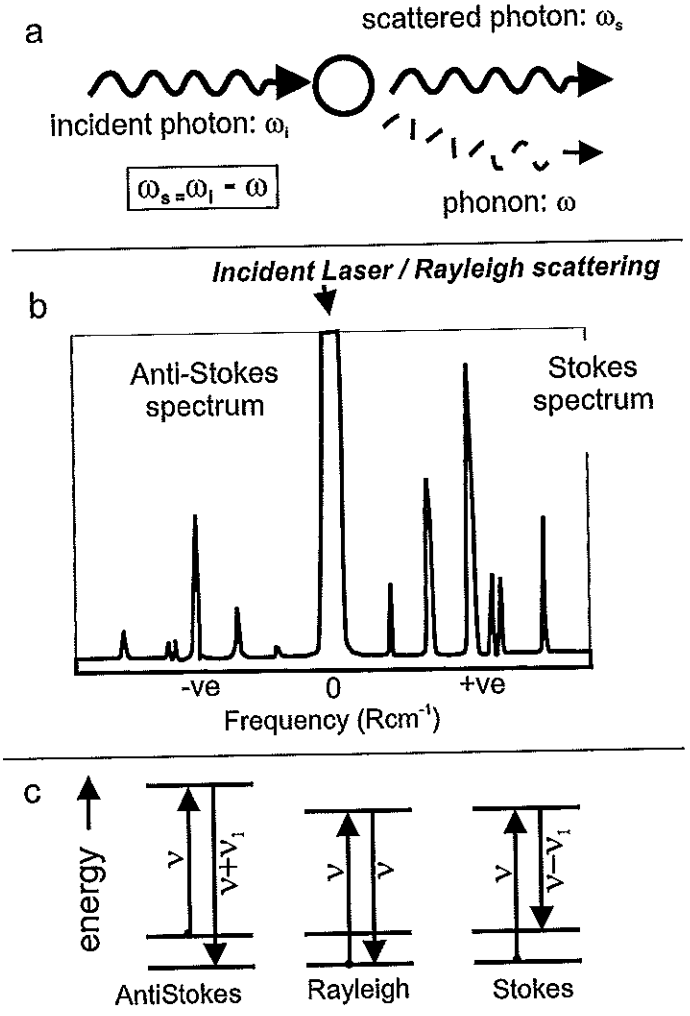

Figure 1 a) Incidence of a photon on a sample creating a new photon and a phonon. b) Raman spectrum: the Raman effect causes changes in the frequency of the incident light, resulting in a spectrum. The frequency shifts may be either positive (Stokes) or negative (antiStokes). c) Energy level diagram illustrating the changes in vibrational energy that result in the spectrum.

The Spectrum

Vibrations in simple molecules

Some simple examples of common molecules will be considered, using the classical model, to show how the bond vibrations result in Raman peaks.

For the simple diatomic molecule of the gas N_2, (Figure 2a) there is no permanent dipole moment, and as the single mode of vibration (N-N stretch) is totally symmetrical, no change in the dipole moment occurs during the vibration, which is therefore infrared inactive. However, the molecule does have a polarizability, and as the N-N bond stretches, the polarizability will change: this vibration will therefore be Raman active.

For polyatomic molecules the total dipole moment or polarizability will be made up of individual bond dipoles or bond polarizabilities. Vibrations will involve stretching and/or compression of more than one bond, and the Raman or infrared activity will depend on how all of these fit together. The vibrations usually described are known as "normal vibrations", that is the simplest combination of individual vibrations which together describe the vibration state of the entire molecule.

The gas CO_2 is a linear symmetric molecule (O-C-O). It has three classes of vibrations (Figure 2b). For the symmetric O-C-O stretch, no dipole is created as the molecule remains symmetrical and it is therefore infrared inactive. However, the polarizability does change, and this vibration is Raman active. For the asymmetric stretch the symmetry is different at each end of the stretch, creating a difference in the dipole moment, and the vibration is active in the infrared. However, the polarizability at each end of the vibration cancels out, resulting in the vibration being Raman inactive. A third type of vibration is a bending around the central C atom. There are two bends that occur, at right angles to each other (i.e. within, and perpendicular to, the plane of the page). Both these bends will have the same frequency, and form what is known as a degenerate pair: only a single peak will be seen in the spectrum. However, although the bending forms dipoles perpendicular to the molecular axis making it infrared-active, the polarizability derivatives are zero and the bend is Raman inactive.

The water molecule H_2O is non-linear (Figure 2c). In this case the vibrations are no longer simply bending or stretching, but are predominantly one or the other. There are, again, three vibrations: a predominantly symmetric stretch, a symmetric bend, and an asymmetric stretch. In this case, all the vibrations cause changes in the polarizability, and all are active in both infrared and Raman. Note that the predominantly bending vibration occurs at a much lower frequency than the stretches.

The importance of symmetry

For more complex molecules, simple inspection cannot predict all the vibrations and their Raman or Infrared activities. However, whether or not a bond vibration will cause a change in the polarizability will depend on the symmetry of the molecule. Thus for more complex molecules the molecular or crystal symmetry must be considered, and the mathematical method of group theory can be applied to predict the number of normal vibrations and their activity in the Raman or Infrared. A useful and relatively simple explanation of crystal symmetry and group theory as applied to spectroscopic analysis is given in the chapter "Symmetry: its description and consequences", in Atkins (1990).Tables detailing the Raman activities of all the different symmetry groups are widely available (e.g. Nakamoto, 1986).

One of the uses of predicting the numbers of Raman peaks is in determining the structure of a molecule. For example, a molecule of composition AX_4 may have either a square-planar or a

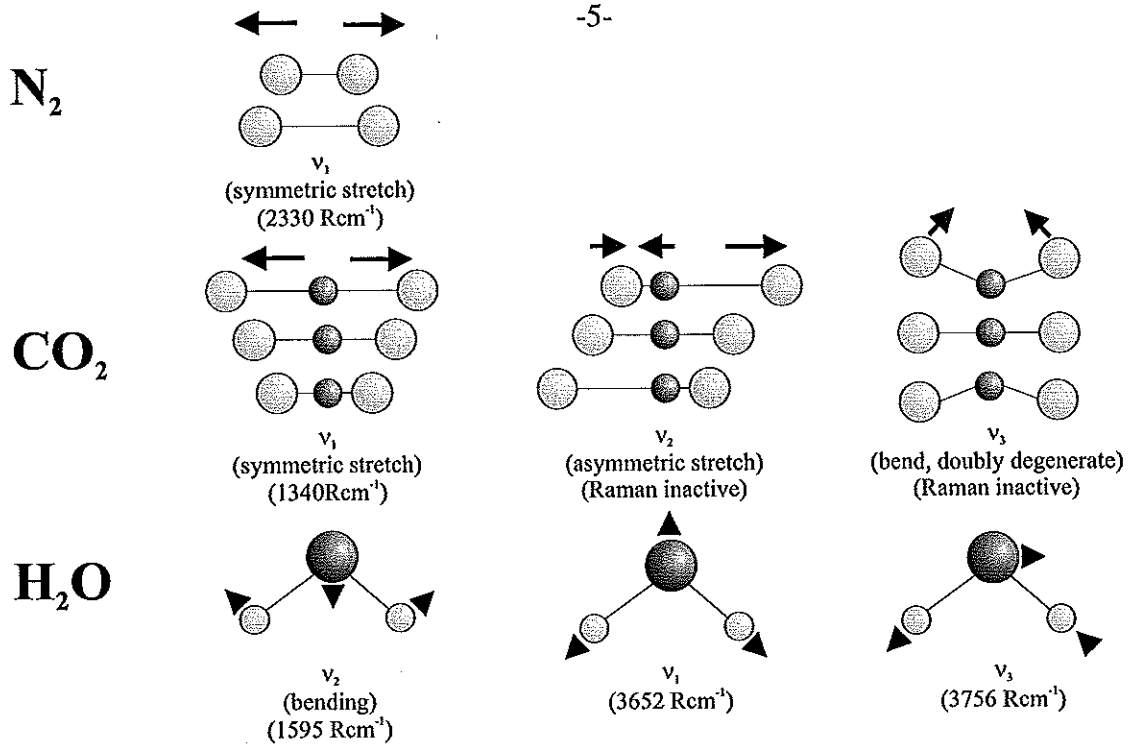

Figure 2 a) Molecular vibrations for the diatomic molecule N_2 b) the linear symmetric molecule CO_2 c) the non-linear molecule H_2O

tetrahedral structure (Fig. 3). The square-planar structure, with symmetry class D_{4h} would be expected to show three Raman bands[1], while the tetrahedral structure, symmetry class T_d should show four Raman bands. Thus, the spectrum will allow the determination of which structure is present. It should be noted, however, that the if a band is not observed, it does not necessarily mean it is not present: some bands have low intensities and may not be observed except in very clear spectra.

For molecules with a centre of symmetry all vibrations will either be Raman *or* Infrared active: they cannot be both (this is the mutual exclusion rule).

---

[1] **Footnote: terminology**

Papers describing Raman data often contain some confusing terminology, which must be explained briefly. Usually the molecule of interest is described in terms of its symmetry. The symmetry is most commonly described using Schönflies notation (e.g. $D^{19}{}_{4h}$, C_{2v}) which indicates the symmetry elements needed to define the overall symmetry of the molecule. For example, a symmetry group C_{2v} has a single rotation axis (C) which is two-fold, and a vertical reflection plane. The symmetry groups are fully described in references such as Atkins (1990) or Nakamoto (1986).

The vibrations are described in two ways: terms such as A_{1g}, A', or E_u are known as Mulliken symbols relate to a character table of the symmetry operations for the molecular point group. They describe the symmetry of the vibration: for example, A_{1g} vibrations are always totally symmetric, and E vibrations are generally degenerate (i.e. 2 or more equivalent vibrations occurring in different directions, but all having the same frequency, resulting in a single peak).

Within a spectrum, peaks are often referred to as ν_1, ν_2, etc. The order depends on the symmetry of the vibration, and the frequency of the peak. Thus, ν_1 will always represent the highest frequency mode of the most symmetric species.

Individual vibrations are often referred to by symbols such as ν(C-O). This represents the type of vibration: ν (A-B) represents bond stretching between the two atoms, while δ(A-B-A) represents bending around the central atom.

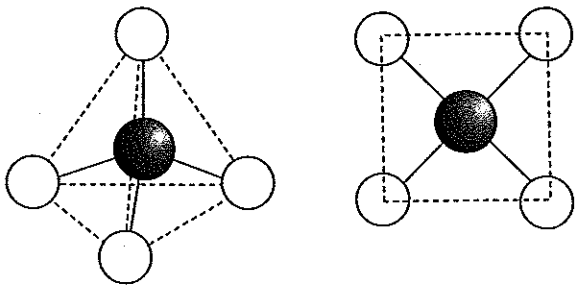

AX_4

	Tetrahedral	Square planar
Structure:		
Symmetry group	T_d	D_{4h}
Symmetry operations	$4C_3, 3C_2, 6\sigma_d, 6S_4$	$C_4, 4C_2, \sigma_h, 2\sigma_v, 2\sigma_d\ 2S_4, I$
Raman Vibrations	$A_1, E, 2F_2$	A_{1g}, B_{1g}, B_{2g}
No. of Raman peaks	4	3

Figure 3: The difference in symmetry and therefore in the number of bands in the Raman spectrum for two possible structures of a molecule AX_4: the tetrahedral form should show four Raman peaks, while the square-planar form should show only three.

Effects of different phases

Although one of the advantages of Raman analysis is that it may be used on a variety of different phases (gas, liquid, single crystals, powder...) different phases may show very different spectra.

Free molecules in a gas will tend to show finely spaced lines, at small frequency shifts, due to rotational effects: these lines occur close to exciting line and require high resolution, as under low resolution they appear as relatively broad peaks or a shoulder on exciting line. Other lines may occur at higher frequencies, due to vibrational or vibrational/rotational transitions.

In liquids rotation is inhibited and only vibrational peaks are seen. These will have slightly different frequencies to those for the same molecule as a gas (due to environmental perturbation of energy levels).

Solids have much more complicated Raman spectra, due to the effects of long-range order. Molecular crystals will usually show peaks at high frequencies due to intramolecular vibrations (internal modes), and at lower frequencies due to intermolecular vibrations, translation and rotation, known as lattice or external modes. The spectrum is highly dependent on crystal symmetry and the strength of intermolecular interactions. In single crystals the spectrum also varies with the direction of observation relative to the symmetry.

The Raman spectrum consists of a number of peaks, depending on the substance analysed. For solid samples, the width of the peaks is often indicative of the order within the molecule. For example, quartz has a spectrum showing a number of relatively sharp and well-defined peaks, whereas quartz glass, which has the same composition but no crystal structure, shows a number of broad features (Fig. 4). Similarly, three forms of carbon are illustrated in Figure 5. Diamond shows a single sharp strong peak at 1330 Rcm-1. Graphite shows a much wider peak at 1575 Rcm^{-1}, although the width varies with the crystallinity, from low and broad for disordered graphite to strong and narrow for well crystallised graphite. Amorphous carbon shows a low broad peak at around 1350 Rcm^{-1}, which again varies in shape depending on the degree of order or disorder.

The intensity of a Raman peak is generally proportional to the concentration of the scattering species (assuming that intermolecular interactions don't cause a departure from a linear relationship). Thus where two species are present, such as a mixture between two oxides, then

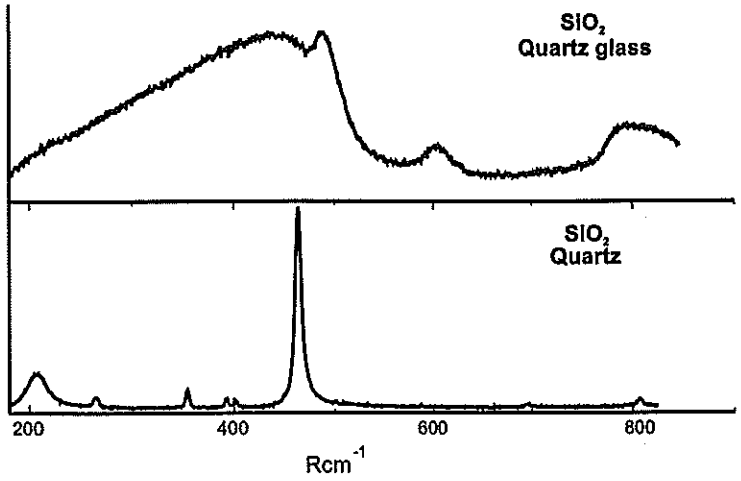

Figure 4: Raman spectra of quartz and quartz glass showing the difference in spectrum between two substances of identical composition but different structure.

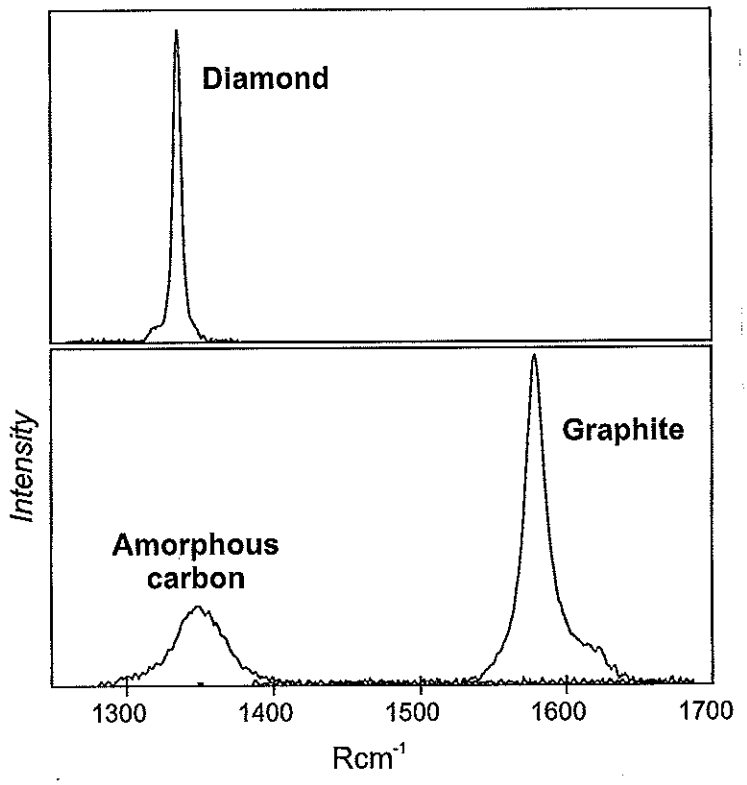

Figure 5: Raman spectra of 3 different forms of carbon: diamond, graphite and amorphous carbon.

the relative intensities of the main peaks for each one will be directly related to the relative proportions. It is this property which allows the determination of the relative proportions of gases in fluid inclusions, described in a later section. However, the intensity of the peaks will vary between different species, and the technique can only be used for direct comparison of composition once the relative intensities have been calibrated for the system under consideration. Additionally, in crystalline materials orientation effects will influence the intensities of the peaks:

comparison of relative proportions is more useful in fluid or finely powdered samples where the grains are randomly oriented.

Knowledge of the symmetry of a molecule allows the determination of which vibrations will be Raman active, but the frequency and intensity of a Raman band depends on the mechanical and electrical properties of molecule, masses and force constants. The conditions of observation and resolution of the instrument also affect the observed spectrum. For example, a number of narrow close bands will appear as a single, wide band if the instrument resolution is poor.

Solids and crystals

In general, the higher the symmetry of a molecule, the simpler the spectrum. However, as the symmetry is lowered by a molecule becoming more complex, more frequencies will occur, but many of them may be inactive. Distortion of a crystal lattice by incorporation of impurities (e.g. substitution of a small proportion of one cation by a different one) will retain the same structure but lower the symmetry.

The symmetry group may vary between a molecule when it is free or when it forms part of a larger molecule or crystal. Generally, the symmetry is lowered, which results in changes in the spectrum: degeneracies will be removed resulting in splitting of peaks, and some peaks may become inactive, but it is more likely that inactive peaks will become active.

The interpretation of Raman spectra is simplified by the fact that functional groups often have characteristic frequency ranges, and the position of a peak within that range provides information on the structural environment. This is particularly useful in organic compounds, where groups such as >C=C<, -C≡C-, or -N=N- have characteristic positions. Similarly, in silicate minerals the Si-O stretches fall into one range, and the O-Si-O bends into another. In the same way, sulphates or carbonates will show peaks in a characteristic range due to intramolecular vibrations in the free CO_3^{2-} or SO_4^{-} anion. These will differ slightly in frequency, depending on the surrounding environment (i.e. the type of cations involved, and the crystal structure). The spectra will also show a number of peaks representing inter-molecular vibrations (Fig. 6).

The structure of a mineral has a more important effect on the Raman spectrum than the actual composition. For example, in silicates, the main peaks come from bonds within and between tetrahedra, and these will vary depending on the degree of polymerisation of the silica molecules. Thus feldspars will show a very different spectrum from olivines or amphiboles. Within a group, the different cations will have a more minor but still significant effect on the peak positions, allowing interpretation of the composition. This technique was used by Mernagh (1991) to distinguish between feldspar minerals.

Although the spectra of complex molecules can be hard to interpret, there are a few general rules which can help. The frequency of a stretching vibration depends on the masses of the atoms involved: higher masses will end to have lower frequencies, but higher intensities. Stretching vibrations will tend to be more intense, and usually at higher frequencies, than deformations vibrations. Multiple bonds such as C=C will tend to have more intense stretching peaks than single bonds (C-C) between the same atoms.

The symmetry of an individual molecule is described in terms of its point group symmetry, which is usually relatively simple. However, when a molecule or ion is incorporated into a crystal the Raman spectrum will depend on the longer-range structure within the crystal, and the surroundings must therefore also be considered. Two approximations for the overall symmetry may be used: the Site Group approximation, which considers the symmetry of the site within the crystal (for example, considering a CO_3 unit in a carbonate as occurring at a single site); and the Factor Group approximation, which considers the symmetry of an entire unit cell.

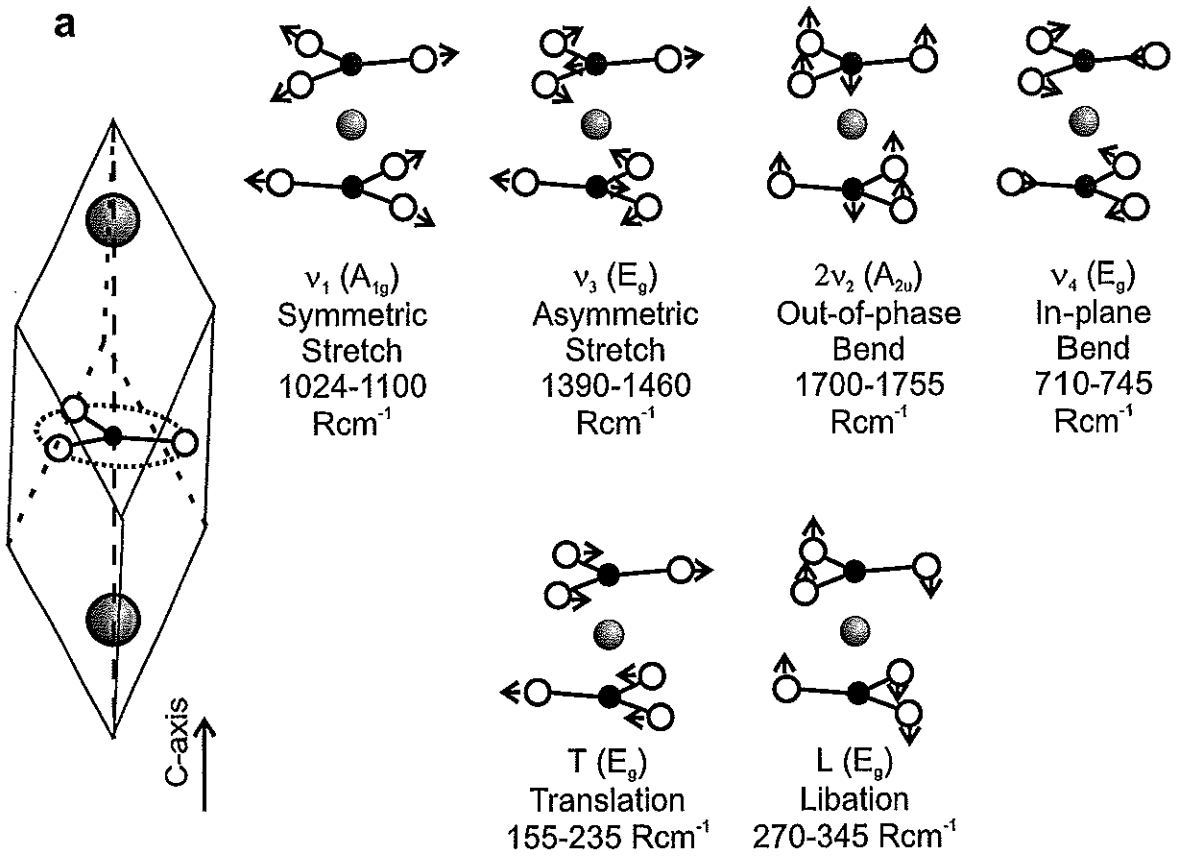

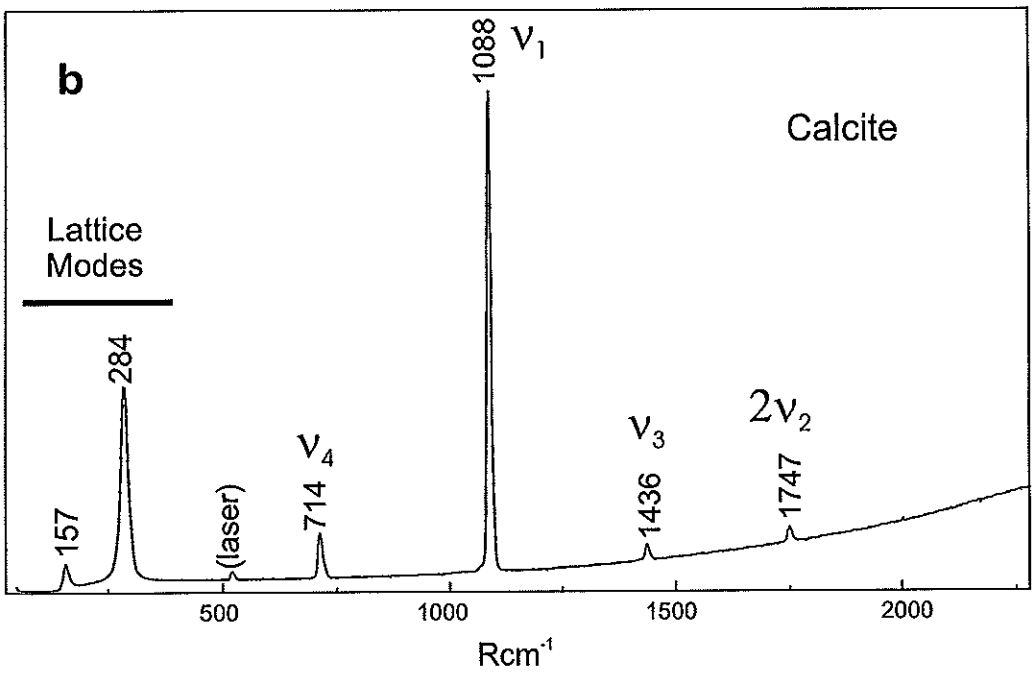

Figure 6: a) The structure of the calcite Bravais primitive cell together with the Raman active vibrations. There are four internal vibrations for the CO_3^{2-} unit, and two translation or libation modes which occur only within the crystal (after Nakamoto, 1986).
b) Raman spectrum for calcite

The spectrum of a unit within a crystal may not deviate observably from that of the free molecule: this depends on how strongly the structural unit or ion interacts with the surroundings. Two main effects that can occur are changes in the selection rules, and splitting of degeneracies.

Selection rules determine whether or not a vibration is Raman active. A given vibration may be inactive when the symmetry is that of a single molecule (point group symmetry), but become active in the lower site group symmetry. For example, the A_1' mode in the CO_3^{2-} ion , due to a C-O symmetric stretch, is not infrared active in the D_{3h} symmetry of the free ion. When the ion is incorporated into a calcite crystal, the site symmetry for the CO_3^{2-} ion is D_3, and the A_1' vibration mode is still not infrared active. However, if the same ion is incorporated into a crystal of aragonite, the site symmetry becomes C_s, and in this symmetry the A_1' becomes infrared active.

As described earlier, certain vibrations may be degenerate, that is two or more vibrations have the same frequencies, and will be represented by a single peak. However, the lowering of symmetry as a molecule is incorporated into a crystal may result in the splitting of a degeneracy, so that the vibrations no longer have the same frequency and two separate peaks are observed. To take again the example of $CaCO_3$, in calcite the two vibrations ν_3 and ν_4 are degenerate and are each seen as single peaks. In aragonite these degenerate vibrations split. However, magnitude of splitting may be too small to be observed, depending on resolution.

Another example of this effect is in a linear ion, similar in structure to the CO_2 (O-C-O) molecule described earlier, which has two bending vibrations. These bends occur at right angles to each other and are doubly degenerate, since bending in any plane is equivalent to bending in any plane perpendicular to it. However, inclusion of such a linear ion in a crystal lowers the overall symmetry and may prevent those planes from being equivalent, resulting in splitting of these single peaks.

Polarisation and orientation studies

The polarisation characteristics of the scattered light are often different from the incident light, and the intensity and polarisation of scattered light depend on the direction of observation.

Polarisation studies can help to determine which peaks in a spectrum represent which vibrations. For example, symmetric vibrations do not change the polarisation character of the incident light by much, and the resultant scattered light will be greatly reduced when observed with a polarisation perpendicular to the incident polarisation (Fig.7). Non-totally symmetric vibrations will change the scattered light polarisation, and there will be less difference (in some cases virtually no difference) between the scattered light observed with polarisation perpendicular or parallel to that of the incident light. Unfortunately, the nature of the optical set up means that polarisation studies cannot usually be carried out using a microscope.

Raman analysis of single, oriented crystals can provide excellent information on the structure by examining the spectrum and its polarisation characteristics for each crystal face (Fig.8). However, for most Raman studies a finely powdered sample is preferable. If larger crystals are not in a known orientation, the differences in spectra between differently oriented crystals can confuse the identification. Analyses of finely powdered samples offer a random sample of orientations, as for X-ray powder diffraction, and therefore provide a more characteristic and representative spectrum.

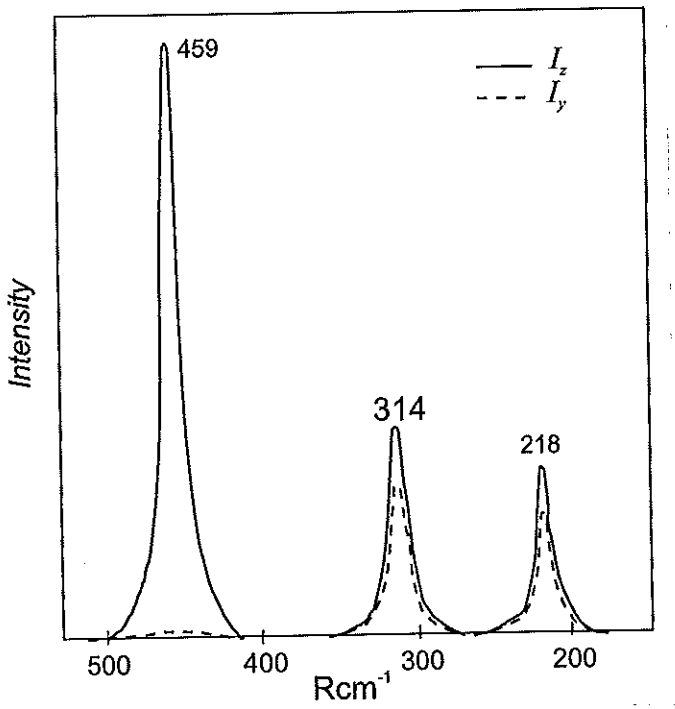

Figure 7: Polarised spectra of CCl_4 showing the effect of two different polarisation orientations (from Nakamoto, 1986). The peak at 459 Rcm^{-1} is polarised, showing a large decrease in intensity with changing polarisation: this indicates that it is totally symmetric.

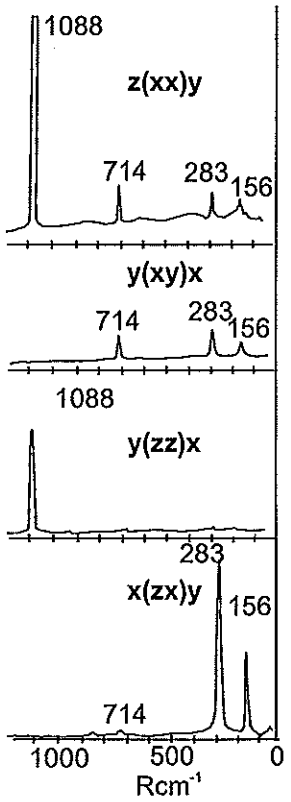

Figure 8: Polarised Raman spectra from different orientations in calcite (from Nakamoto, 1986), showing how the spectrum changes with crystal orientation. The peak positions remain the same but their intensities vary, and in some cases a peak may not be observed.

EXPERIMENTAL AND INSTRUMENTAL CONSIDERATIONS

Raman Spectrometers

Any Raman system involves the focusing of light onto a sample, collection of the scattered light, dispersal of the light into separate wavelengths, and a detector to register that light (Fig.9).

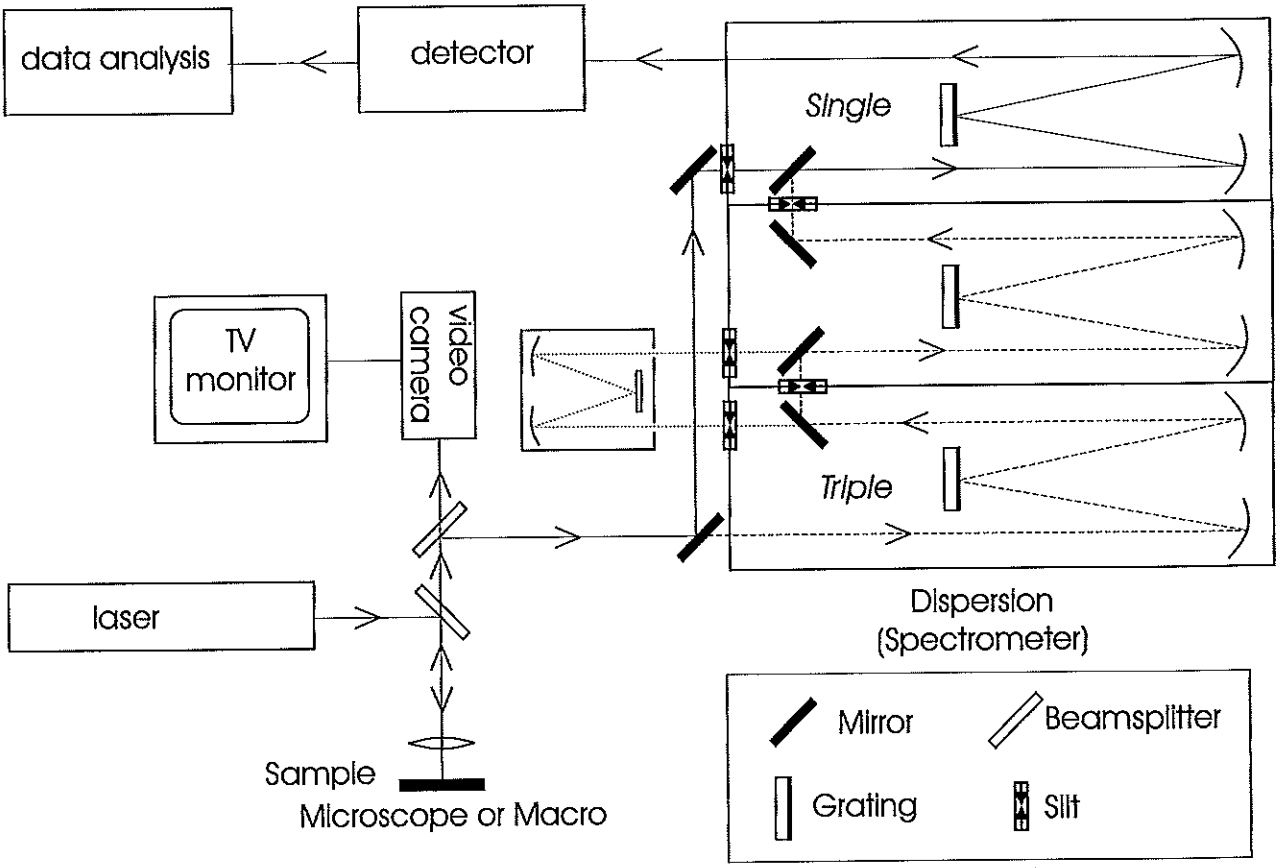

Figure 9: Diagram of a typical Raman set up, showing the various elements described in the text.

Light source

As the intensity of Raman scattered light is extremely low (10^{-6} times the intensity of the incident light), a very intense light source is required. In addition, the light source needs to be monochromatic, and often plane polarisation must be applied. In the past the light source was often a halogen or mercury lamp, but now it is almost always a laser. Lasers have the advantage of a very high intensity in a small area, and are generally monochromatic. A wide range of wavelengths is available: the most commonly used is probably the argon ion laser, with strong outputs at 514nm (green) and 488nm (blue). Other lasers such as helium-neon or krypton are used when fluorescence characteristics of the sample cause problems: using incident wavelengths in the red range can overcome these problems. For resonance Raman experiments, tuneable dye lasers are used.

Sample

Usually two possible sample stage options are available. The "macro" option is used when large, or liquid samples are used, or when bulky equipment such as a furnace or cryostat is required. Also, for single crystal polarisation studies, the macro mode is most useful. For most geological applications, however, a microscope is used. The laser is focused, and the scattered light collected, through the objective of a normal research microscope, and the sample can be viewed and precisely positioned under the microscope. The microscope lens focuses the beam so that a spot as small as 1μm is analysed, and use of confocal optics reduces the depth of the focal barrel, rejecting light from outside the desired area, so that thin layers or small inclusions within a larger sample can be analysed. Using a motorised microscope stage, maps or traverses can be made. Focusing of the laser light down to such a small spot means that the laser power is very intense, and care must be taken that the sample is not damaged. This can be particularly important for dark coloured or opaque samples, which absorb the laser light.

Filters

A number of filters are employed in the system . These may include an interference filter before the sample to reject plasma lines from the laser, a holographic filter after the sample to remove the reflected and Rayleigh scattered laser light, and various polarizers and half-wave plates to adjust the polarisation of the light both before and after the sample.

Dispersion

The scattered light must be dispersed into its separate wavelengths, in a manner similar to that of a prism splitting sunlight into its separate colours. This is done via a system of holographic diffraction gratings, which may be used singly or in series depending on the experiment in question. A range of grating are available, allowing rapid analysis of a wide spectral range but at relatively low resolution, or a much narrower range at higher resolution. Again, the choice of system will depend on the sample and problem in hand, but modern Raman systems allow rapid changing between different settings to allow flexibility.

Detectors

The light is then recorded using a photo-sensitive detector. The most common types are a single channel photomultiplier tube (PMT) which used to be the most common detector, but is now used only in certain situations, such as when very high resolution is required; and a multichannel charged coupled device (CCD). The latter is much more rapid, allowing a wide range of wavelengths to be detected simultaneously, and liquid nitrogen cooling results in a very low background or dark signal.

The spectrum is then read from the detector via computer software.

APPLICATIONS OF RAMAN AND LUMINESCENCE STUDIES IN GEOLOGY

A number of the applications of Raman spectroscopy in geology will be described with examples. Recent reviews of Raman spectroscopy in the Earth Sciences include those by McMillan (1989) and Roberts and Beattie (1995).

Fluid Inclusions

Probably the most commonly used geological application of Raman spectroscopy is in the study of fluid inclusions. Fluid inclusions are tiny bubbles of fluid trapped in a crystal as it forms, or within fractures in the crystal, where inclusions are trapped as the fracture is healed. In most cases we can assume that the volume and composition of the inclusion contents has not changed since it was trapped, and the inclusion can be considered as a sample of the fluid which was present at the time of formation of the inclusion.

Fluid inclusions typically contain water, with various dissolved salts such as NaCl, gases such as CO_2, N_2, CH_4, and commonly salt crystals, which were soluble at the high temperature when the inclusion formed, but are no longer soluble. In fact, the gases were usually also dissolved at high temperature, and there was no vapour bubble present, but as the fluid has cooled and the crystal around it contracted, the fluid has separated out into different phases.

Fluid inclusions can be used to provide important information about the physico-chemical conditions prevalent at the time of formation of the bubble. Typically they are used to provide information on metamorphic or igneous fluids, or on hydrothermal fluids involved in mineralising or vein-forming episodes. Using microthermometry, the minimum temperature at which an inclusion was trapped can be determined, and if the composition of the fluid is known pressure-temperature conditions can be calculated.

The most common use of Raman in fluid inclusions is to measure gas composition. The laser is focused directly inside the fluid inclusion, into the gas or vapour bubble, and if gases are present they will show characteristic peaks in the spectrum (Fig.10). The spectrum of quartz (or any other host mineral) will also be present, but does not usually interfere. The species most commonly described are CO_2, CH_4, N_2, more rarely H_2S, C_2H_6, C_3H_8, and even more rarely SO_2, CO, H_2, O_2 and NH_3.

The relative concentrations of the gases can be calculated by comparing the area under each peak. However, some gases have much stronger Raman intensities than others do, so it is necessary to apply a correction factor. For most common gases these factors are known and published.

Some of the earliest reports of the use of Raman analysis for fluid inclusions were those of Rosasco *et al.*, (1975) and Dhamelincourt *et al.*, (1979). A useful review of the use of Raman spectroscopy for fluid inclusion analysis is given by Burke, (1994). A review of some of the advances in our understanding of fluids as a result of such analyses is given by Dubessy *et al.*, (1989).

Other factors can also be determined from the Raman spectrum. For example, the position of the CH_4 peak varies with pressure and with careful calibration this can be used to determine the internal pressure (Chou *et al.*, 1990; Fabre and Oksengorn, 1992; Seitz *et al.*, 1993). The shape of the 1388 CO_2 peak can also indicate the presence of $^{13}CO_2$, as a small shoulder on the low frequency side: the increased mass of the ^{13}C isotope relative to ^{12}C slightly reduces the frequency of the peak (Dhamelincourt *et al.*, 1979). It is possible that in future this effect may be calibrated allowing an estimate of the relative proportions of $^{13}CO_2/^{12}CO_2$. Fully quantitative

analysis of gases (i.e. calculation of the absolute concentration, rather than just the relative concentration) is difficult, due to effects such as presence of the surrounding host mineral on the absolute scattering efficiency, combined with the character of the individual instrument (Pasteris *et al.*, 1988; Wopenka and Pasteris, 1986).

Hydrocarbons can also be detected in this way and estimation of the chain length can be made (Pironon, 1993).

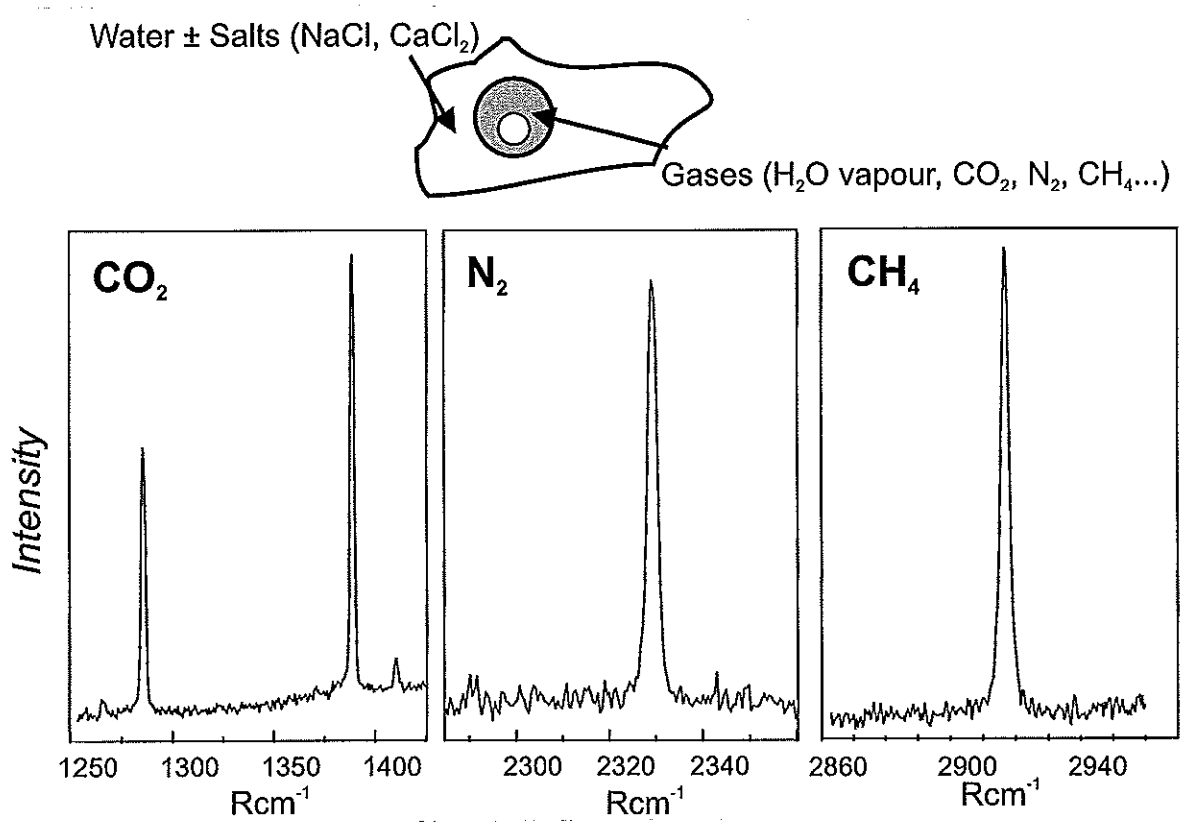

Figure 10: Illustration of a fluid inclusion showing aqueous solution, with immiscible bubble of liquid CO_2 +/- N_2, CH_4; vapour (containing gases and water vapour. The laser is focused inside the bubble, resulting in a Raman spectrum, showing CO_2, N_2, and CH_4 peaks.

Complex ions in solution, such as carbonate and sulphate ions, can also be detected by Raman spectroscopy (e.g. HS^-, HSO_4^-, SO_4^-, and NH_4^-). Simple ions in solution (such as Na^+, Cl^-) cannot be detected by Raman spectroscopy: they form no bonds , so no bond vibrations occur. (In fact, they may form vary weak hydrogen bonds with water molecules but these are not strong enough to give detectable Raman peaks). However, at low temperatures (such as during the freezing cycle of microthermometry) some salts and gases react with water to form solid hydrates. These hydrates do show Raman spectra, and although the use of Raman to identify them is not common, it has possibilities (Dubessy *et al.*, 1992).

Some daughter minerals (salts which have precipitated out of the solution) or trapped phases (solids which were caught in the inclusion when it formed) can be identified by Raman spectroscopy. The most common daughter mineral, sodium chloride NaCl does not have a

Raman spectrum, since it is ionic in nature and does not have any real bond to allow vibration. However, other minerals such as carbonates, or barite do show spectra.

During low temperature microthermometry, gases will react with water to form solid gas hydrates or clathrates. These clathrates are difficult to see, due the similarity between their refractive index and that of water. They can affect the microthermometric measurements at low temperature. These clathrates show Raman spectra: the peak position of the gas is shifted to a slightly lower frequency due to the entrapment in a solid lattice. Raman analyses can provide important information on the phase relationships and composition of these clathrates (e.g., Seitz and Pasteris, 1990; Seitz *et al.*, 1987). Raman analyses of the clathrate and the residual fluid has shown that differential partitioning of gases between the fluid and solid phases may concentrate trace gases such as N_2 into the remaining fluid. At the temperature of melting of CO_2 the gas may therefore be artificially enriched in N_2 relative to CO_2 (Murphy and Roberts, 1995; Murphy and Roberts, 1997). Microthermometry will therefore give an erroneous estimate of gas composition, making it even more important to analyses the gases directly by Raman spectroscopy.

Minerals

Silicates

The spectra of silicates generally represent the linkage of SiO_4 or AlO_4 tetrahedra. The Si-O stretching frequencies tend to increase with the degree of polymerisation of the silicate structure (White, 1975), and the O-H stretching frequency can be useful for locating -OH groups in hydrous minerals. Silicate spectra are typically complex, but it is generally possible to differentiate between different silicate groups (e.g. Griffith, 1975) or within groups, for example the feldspars (Mernagh, 1991).

Using a remote optic-fiber probe, Wang *et al.* (1995) suggested the use of Raman spectra for identifying minerals during robotic lunar missions. They showed that the spectra of mineral groups such as olivines, feldspar, amphiboles and micas were sufficiently different to distinguish the mineral group and, in certain cases, to distinguish between different mineral compositions.

Sulphides

Sulphide minerals may also be analysed by Raman spectroscopy. Mernagh and Trudu (1993) published a study of a variety of common sulphide minerals including iron and copper sulphides, and sulphosalts. They found that the spectra were distinct enough not only to allow discrimination between different minerals, but also to distinguish subtle structural differences, for example in pyrites of identical composition. As with other minerals, polymorphs will have distinct spectra and allow, for example, sphalerite to be distinguished from wurtzite, or marcasite from pyrite. However, some minerals, such as galena and pyrrhotite show no Raman spectra, and those which do have spectra are easily heated and damaged by the laser, but this can usually be avoided by careful adjustment of the analytical settings.

Glasses

A large amount of work has been carried out on silicate glasses both on natural samples and during high-temperature laboratory experiments (e.g., Mysen and Frantz, 1993; Daniel *et al.*, 1995). The spectrum of a glass is generally characterised by relatively broad features (Fig 4) but it is possible to determine a certain amount of the structure (for example, whether structural groups such as SiO_3^{2-} or $Si_2O_5^{2-}$ are present. Glasses of other compositions, such as carbonates, have also been studied (Genge *et al.*, 1995)

Mineral Polymorphs

As Raman spectroscopy studies the structure, rather than the composition of a sample, it can be used to distinguish between mineral polymorphs. For example, it has been used to distinguish calcite from aragonite in fossils, (e.g. Roberts and Murray, 1995) and in metamorphic terranes, where aragonite is an indicator of high-grade conditions. Similarly, silica polymorphs such as coesite, stishovite and cristobalite can be easily recognised (e.g. Kingma *et al.*, 1995; Palmer *et al.*, 1994), providing important information on metamorphic conditions.

Graphite and Carbonaceous Matter

the Raman spectrum is sensitive to the degree of order in a material, and as described earlier, the Raman spectrum of graphite and amorphous carbon changes with the crystallinity of the sample. This has been used by Pasteris and Wopenka (1991) as an indicator of the degree of metamorphism. Graphite is common in metamorphic rocks, as a result of transformation of organic matter in the original sediments. The crystallinity of the graphite will increase with the grade of metamorphism, but will often not be affected by retrograde processes, reflecting the peak metamorphic conditions. Pasteris and Wopenka (1991) found that they could classify metapelite samples into chlorite, garnet, staurolite and sillimanite zones, and rank samples within those zones, by comparing the position and intensities of the amorphous carbon peak at ≈ 1360 Rcm^{-1}, the graphite peak at ≈ 1580 Rcm^{-1} and the second-order peaks in the region around 2700 Rcm^{-1}. (Fig. 11)

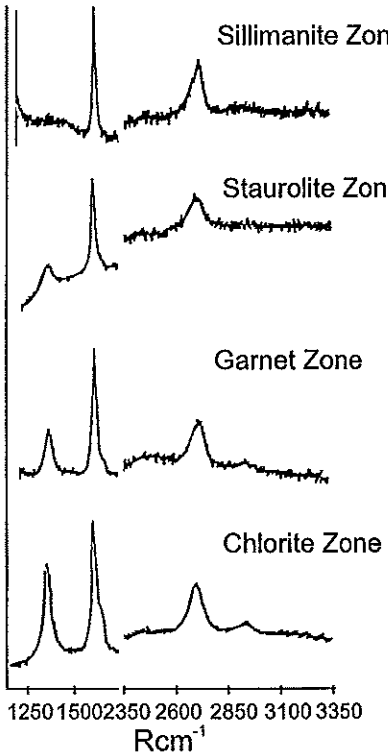

Figure 11: Raman spectra illustrating the increased crystallinity of graphite, moving from chlorite to garnet, staurolite and sillimanite zones of metamorphism. Spectra from Pasteris and Wopenka (1991).

The effect of temperature and pressure on carbonaceous material has also been used as an indicator of maturation, for example Raman spectroscopy has been used to study chitinozoa (Roberts *et al.*, 1995). This can be useful in determining whether or not a sedimentary rock has undergone the conditions necessary to convert the natural organic matter present into hydrocarbons in the form of oil or gas.

Solid Inclusions

The use of a microscope allows the direct identification of small solid inclusions within minerals, down to a size of one micron or less. These may be in a thin section or within a single crystal: if it is possible to focus on the inclusion using a microscope, it is usually possible to analyse it. However, the host mineral composition may affect the analysis, as certain minerals have high levels of fluorescence, which may make detection of the Raman signal difficult. An example of this application is given by Dao *et al.*, (1996), who used Raman spectroscopy to identify microscopic inclusions of diamond within ruby crystals.

Stress

A common use of Raman spectroscopy is to study the effects of stress or strain on the crystal structure. This technique is frequently used in diamond, where the peak shape and position changes in relation to the applied stress, and this data is of use to manufacturers of synthetic diamond products in assessing the quality of their product (Catledge *et al.*, 1996; McCormick *et al.*, 1997). It is also possible to study the abundance of molecular dislocations within a crystal (Mitsuhashi *et al.*, 1993). The use of a motorised stage for automated analysis allows contoured maps to be built up of the strain across a sample, or around fractures.

Raman spectroscopy can also be used on geological samples to interpret the degree of strain and therefore the stress undergone by a sample. For example, Miyamoto and Ohsumi (1995) used the shift in frequency of peaks in the Raman spectrum of olivine in chondrite samples to estimate the residual stress and therefore compare the degree of impact shock in the meteorites.

High Pressure: Gem Anvil Cells

Because Raman spectroscopy studies the structure of a sample, it can be used to monitor structural changes under a wide variety of conditions. One such use is the study of samples under very high pressure, generated in a gem anvil cell (GAC). In a GAC, two brilliant-cut gems (traditionally diamond but now increasingly cubic zirconia or sapphire) are arranged with a small amount of sample between them at the points (Fig.12). As the gems are squeezed together, very high pressures are generated in the cell cavity between the two gems. Pressures of up to 300kbar can easily be generated. Gillet *et al.*, (1993) reported the use of a diamond anvil cell together with heating by a CO_2 laser to generate conditions of 3.5GPa and 2000K, allowing them to study $CaTiO_3$ perovskite under mantle conditions.

Using a microscope, the laser can be focused through one of the gems into the cell cavity, and the sample studied by Raman spectroscopy, as the pressure is increased. Usually, as the pressure increases a small essentially linear shift in peak positions is observed. However, when a phase change occurs, it will be readily identifiable by the changes in the spectrum. The pressure is monitored by adding a few small chips of ruby to the cavity, as ruby has a very strong laser-excited fluorescence. The wavelength position of the fluorescence peaks is linearly affected by pressure, and this response has been calibrated, allowing an in situ measurement of the pressure at the point of analysis. This technique has been applied to systems such as high-pressure polymorphs of silica (Kingma *et al.*, 1995; Palmer *et al.*, 1994), and the types of phase changes

studied include crystal-crystal, crystal-melt, crystal-amorphous phase, and glass-liquid (Gillet, 1996).

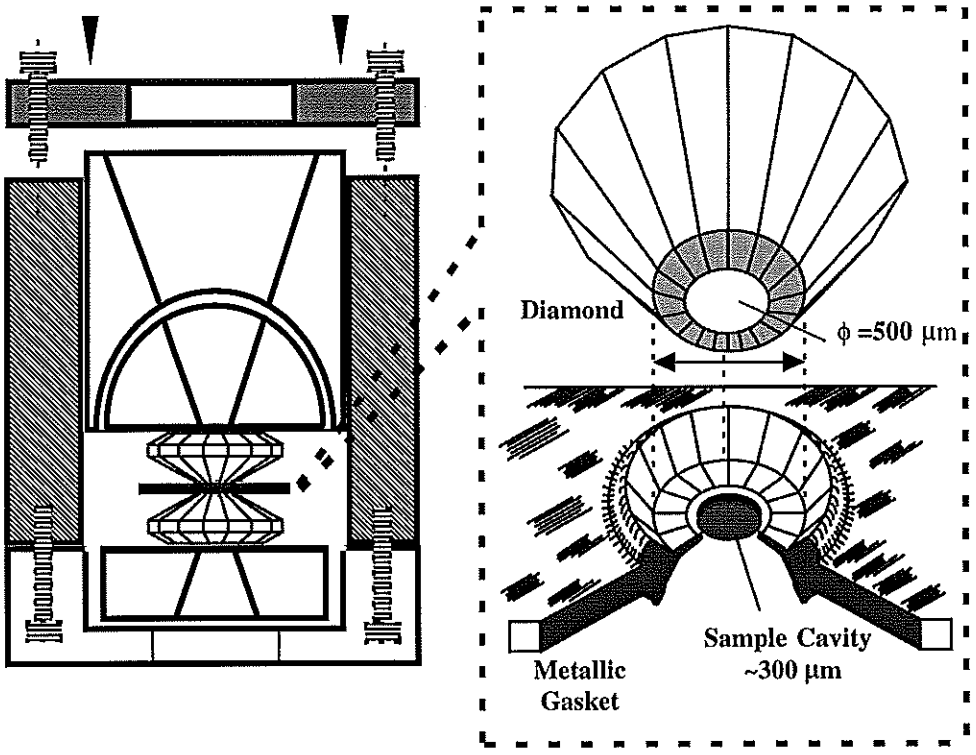

Fig. 12 Illustration of a diamond anvil cell (courtesy Giovanni Hearne, Physics, Wits University)

Study of Surfaces: Oxidation/Corrosion and Mineral Processing

Raman spectroscopy can be applied to the study of oxidation products. This may be either from an experimental perspective, applying certain conditions and then studying the products, or for the study of natural materials. The surface of pyrite under oxidising conditions will form a variety of products, from polysulphides to sulphates, oxides or hydroxides. Such products are often good Raman scatterers, showing clearly distinct spectra (e.g. Mycroft *et al.*, 1990; de Faria *et al.*, 1997; and Fig.13) Although the surface layer may be thin, a layer of 1-2 micron can be easily detected. The mapping facility allows a study of the variation in products across the surface. This can also be used to study iron oxides on corroded surfaces.

In a similar way, Raman spectroscopy can be used in mineral processing, to study the surface of sulphide minerals after reaction. The surface products of the sulphide minerals are extremely important in determining the efficiency of the separation process. Study of the reagents, before and after reaction, and the surface products, allows an understanding of the mechanisms involved. The spectrum may allow the determination of, for example, where in the collecting agent the metal is bonded.

The Study of Gold Speciation in Fluids

An exciting application of Raman spectroscopy is its use for determining the speciation of complexes in fluids. Knowledge of the complexing of metals in fluids is important in developing models for transport and deposition, particularly for gold. Most previous studies on gold complexing have used solubility methods, where the solubility is measured at high temperature, or by quenching the products of high-temperature experiments and calculating the likely

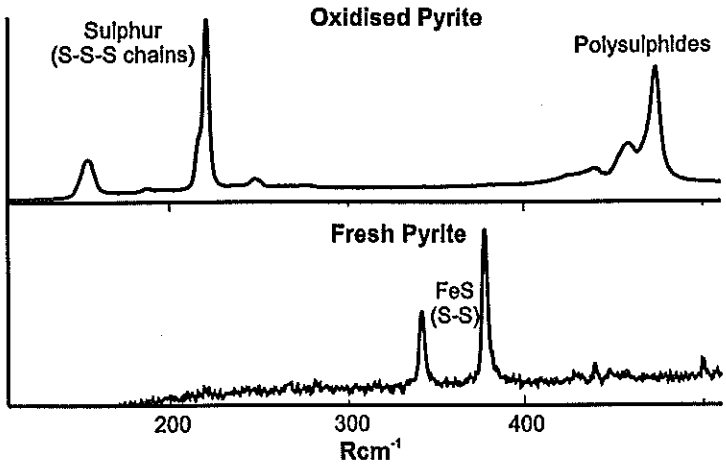

Figure 13: Raman spectra of clean pyrite, and oxidised pyrite showing polysulphide and sulphur peaks. The sample was oxidised experimentally by Paul Holmes (School of Materials and Process Engineering, Wits University).

stoichiometry of the transporting complex. This is useful in providing reaction constants etc..... but does not allow the direct observation of the complex.

Raman spectroscopy does allow direct observation. A great deal of interpretation is still required, but as Raman analyses may be carried out at the temperature and pressure of analysis, rather than on quenched products, it provides an excellent opportunity for the study of complexing reactions.

Most Raman work to date has been carried out on gold-chloride complexes, because of the simplicity of the system and the ease of preparing experimental charges. However, there is no reason why it cannot be applied to hydrosulphide complexes in future.

Development of a hydrothermal cell for studies to 350°c and 2Kbar

Previous Raman work on gold chloride speciation has been conducted at high temperatures but at pressures dictated by the liquid-vapour curve for the system in question. A hydrothermal cell has been developed at the University of the Witwatersrand by Dr Gary Stevens to allow Raman spectroscopic analyses under hydrothermal conditions. A conventional cold seal pressure vessel is used, having been modified to accommodate a conical sapphire window at one end (Fig.14). The laser is focused into a glass sample chamber within the pressure vessel. The fluid sample is isolated from all metallic components, allowing a range of concentrations, and systems, to be studied.

Temperature measurement is via a type K thermocouple (located directly adjacent to the sample capsule) and solid state temperature controller with integral ice point. The pressure-transmitting medium is distilled water, and pressure measurement is by a Bourdon gauge. The cell has been tested to 350°C and 2kbar concurrently. Furnace temperature is controlled by a solid state temperature controller and temperatures at the sample capsule are readily maintained at ±1°C for the duration of an experiment. The laser path length through the fluid is ≈1cm, sufficient to produce good signal/noise even at low concentrations. The sapphire window introduces a number of peaks into the Raman spectrum (Fig.15) but these are narrow and sharply defined: in practice they provide a useful internal calibration of the peak positions for each analysis.

It is anticipated that this apparatus will allow complete study of the Au-Cl system over the hydrothermal range, allowing a much clearer understanding of how the speciation changes with T and P at a range of pH values.

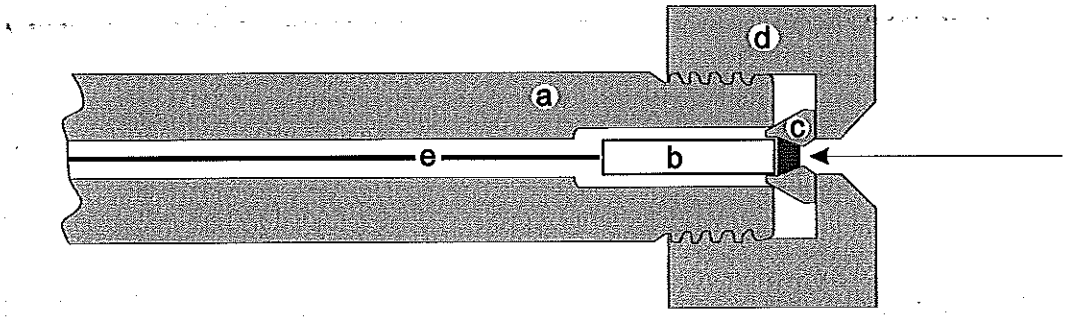

Figure 14: Schematic illustration of the pressure vessel used for Raman experiments. a: pressure vessel, b: glass sample capsule, c: sapphire window holder, d: closure nut, e: thermocouple. The heavily shaded area represents the window and the arrow represents the Raman laser

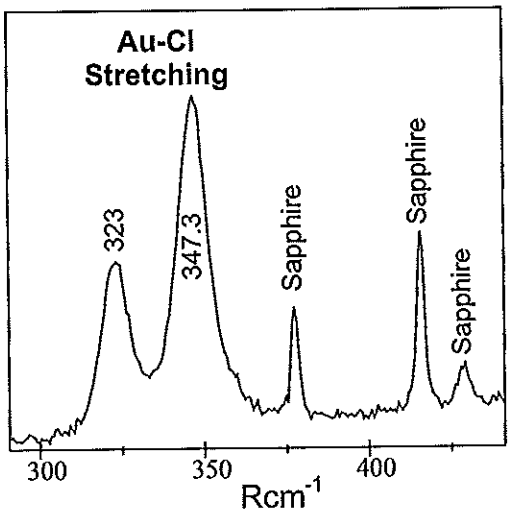

Figure 15: Raman spectrum of $AuCl_4^-$ in the hydrothermal cell sample chamber, showing the occurrence of sapphire peaks.

The use of Raman spectroscopy in the study of metal speciation in fluids will be illustrated by the extended example in Part Two of this Circular. This work has been submitted, in a slightly different form, for publication in *Geochimica Cosmochimica Acta* under the title *Raman spectroscopy of Au chloro-hydroxy speciation in fluids at ambient T and P: a re-evaluation of the effects of pH and chloride concentration,* by P.J. Murphy and M.S. LaGrange

GEOLOGICAL APPLICATIONS OF RAMAN SPECTROSCOPY AND THE USE OF RAMAN SPECTROSCOPY IN THE STUDY OF GOLD SPECIATION IN FLUIDS

PART TWO: A RE-EVALUATION OF THE EFFECTS OF pH AND CHLORIDE CONCENTRATION ON Au CHLORO-HYDROXY SPECIATION IN FLUIDS AT AMBIENT T AND P

INTRODUCTION

An understanding of the behaviour of gold in solution is necessary for models of gold transport and deposition related to the formation of gold deposits. Gold transport in hydrothermal and other natural solutions usually occurs by means of complexation with one or more of a variety of ligands such as HS^- or Cl^-. In such solutions gold is generally present in either the Au(I) or Au(III) oxidation state, although the relative importance of the two under various conditions is still the subject of debate. Similarly, the relative importance of various ligands is debated.

Most experimental work on gold solubility has concentrated either on hydrosulphide complexes (e.g., Renders and Seward, 1989; Shenberger and Barnes, 1989; Hayashi and Ohmoto, 1991; Benning and Seward, 1996) or chloride complexes (Hayashi and Ohmoto, 1991; Farges *et al.*, 1993; Gammons and Williams-Jones, 1995a; Gammons *et al.*, 1997). Vlassopoulos and Wood (1990) studied hydroxide complexes of gold in fluids at temperatures typical of surface waters.

Due to their lower solubility, gold-chloride complexes are likely to be subordinate to hydrosulphide complexes in hydrothermal fluids except where the overall sulphide content of the fluid is low (Hayashi and Ohmoto, 1991). However, many workers consider chloride complexes to be important under certain conditions, such as in highly oxidised fluids of high salinity and low reduced sulphur content (e.g. Shikazono and Shimizu, 1987; Hayashi and Ohmoto, 1991; Gammons and Williams-Jones, 1995b). In hydrothermal systems in which chloride complexes are important, they are likely to be of the Au(I) oxidation state. However, at low temperatures (e.g. below 200°C) Au(III) is likely to predominate over Au(I) (Gammons *et al.*, 1997). Therefore , in fluids such as surface waters hydrolysis reactions of chloride complexes are also likely to be significant.

Although a number of workers have studied speciation in gold chloride solutions (e.g., Farges *et al.*, 1993; Gammons and Williams-Jones, 1995b; Gammons *et al.*, 1997) including two studies using Raman spectroscopy (Pan and Wood, 1991; Peck *et al.*, 1991), some questions remain to be answered. In particular, workers do not always agree on the relative importance of Au(I) and Au(III) complexes or the assignment of peaks in the Raman spectrum to various complexes.

This paper presents a reassessment of the Raman spectra of chloride and mixed chloro-hydroxy complexes of gold and their variation with pH and chloride concentration, in order to resolve differences between the work of Pan and Wood (1991) and Peck *et al.* (1991) and between their experimental data and the theoretical predictions of Tossell (1996).

Raman spectroscopy is an ideal technique for studying gold complexes in solution. Unlike the complementary vibrational technique of infrared absorption spectroscopy, the spectrum of water is unlikely to interfere with the solute spectrum. The peaks in a Raman spectrum represent vibrational modes within the molecule, and can therefore be used as a fingerprint when known

spectra are available, or as a method of determining molecular structure. The vibrational frequencies depend on the atoms involved, bond force constants and the symmetry of the molecule. As a result, different gold complexes will have different Raman spectra, and the number, frequencies and polarisation characteristics of the peaks in a Raman spectrum can serve to identify the species under consideration. For example, for the square-planar $[AuCl_4]^-$ complex, three Raman peaks are observed: two are due to Au-Cl stretching, and one to Cl-Au-Cl bending (Table 1, and Fig. 16). A number of other vibrational modes are either infrared active, or inactive.

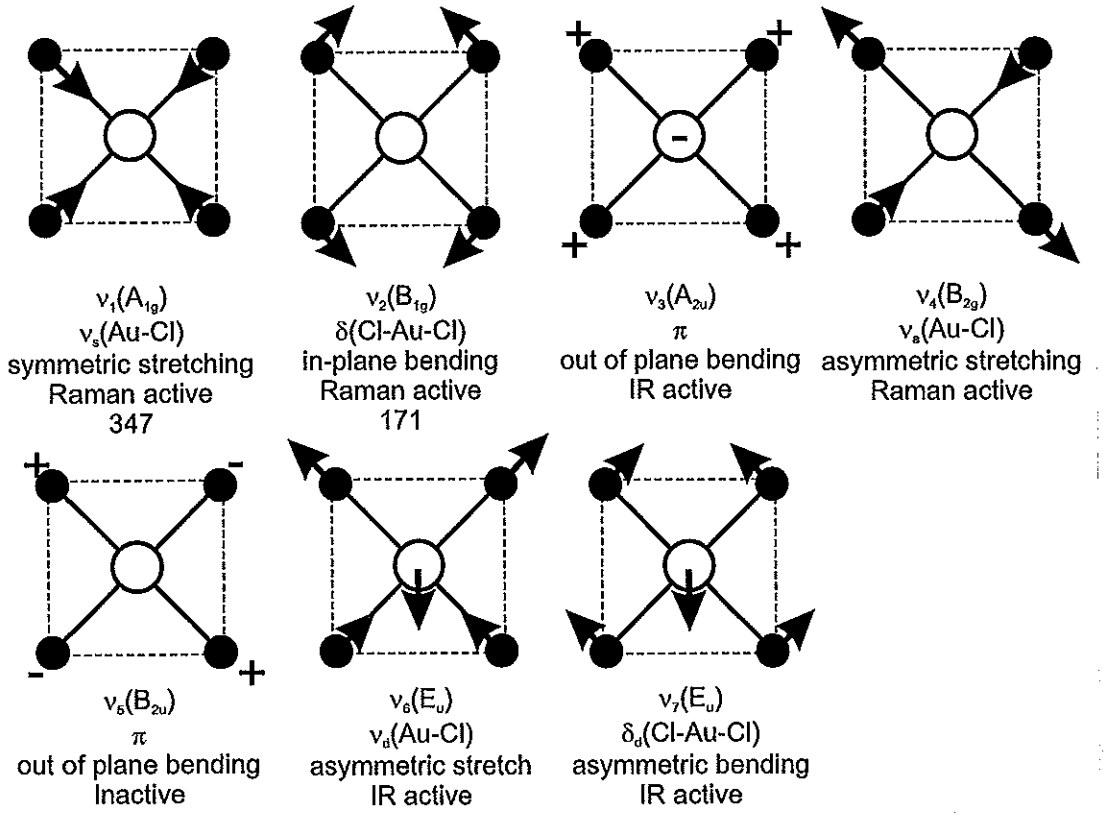

Figure 16: Normal vibrations for the $[AuCl_4]^-$ complex, showing Raman active, Infrared Active, and inactive vibrations.

A hydrolysis sequence of Au(III) complex ions of the formula $[AuCl_x(OH)_{4-x}]^-$ (where x = 0 to 4) and with square-planar geometry is known to exist (Cotton and Wilkinson, 1988). For mixed chloro-hydroxy species, Au-OH bonds are present in addition to Au-Cl bonds, resulting in Au-OH stretching or bending vibrational modes.

PREVIOUS WORK

Gold-chloride speciation in highly acidic solutions was studied by Pan and Wood (1991), using Raman spectroscopy from room temperature to 300°C and at pressures along the liquid vapour curve. They described Raman peaks consistent with the $[AuCl_4]^-$ complex (171, 324 and 347 Rcm^{-1}) at low temperatures, and the introduction of a new peak at 332 Rcm^{-1} above 150°C, which they interpreted as resulting from a partial transformation of $[AuCl_4]^-$ to $[AuCl_2]^-$. This polarised peak was therefore attributed to a totally symmetric Au-Cl stretch in the $[AuCl_2]^-$ complex. The solutions in the study were kept extremely acidic in order to avoid hydrolysis reactions. However, such very acidic solutions are unlikely in geological environments, and

hydrolysis reactions are therefore likely to play an important role in gold speciation in natural solutions.

The effect of pH on gold-chloride complexing was discussed by Peck *et al.* (1991) who studied gold in 1M NaCl solutions at room temperature, using both Raman and UV-visible absorption spectroscopy. They adjusted the pH using HCl and NaOH to a range from 4 to 12.2. At low pH (<5.8) they found similar Raman spectra to the room-temperature analyses of Pan and Wood (1991) for the $[AuCl_4]^-$ complex. As the pH was increased, they reported the appearance of new peaks both in the Au-Cl stretching range around 340 Rcm^{-1} and Au-OH stretching around 570 Rcm^{-1}. They interpreted these peaks to represent successive replacement of Cl^- by $(OH)^-$, in the sequence $[AuCl_x(OH)_{4-x}]^-$, i.e. from $[AuCl_4]^-$ to $[AuCl_3(OH)]^-$, $[AuCl_2(OH)_2]^-$, $[AuCl(OH)_3]^-$ and possibly $[Au(OH)_4]^-$. For each complex after the original $[AuCl_4]^-$ complex Peck *et al.* (1991) found only one Au-Cl stretch , and one Au-OH stretch, until at high pH they reported two Au-OH stretches for both $[AuCl(OH)_3]^-$ and $[Au(OH)_4]^-$. The peak positions reported for these complexes are summarised in Table 1.

		Predicted Raman Vibrations [1]			Predicted Frequencies [3]		Experimental		This Study	
Complex	Space group	Total [1]	Au-Cl Stretch [2]	Au-O(H) Stretch [2]	Au-Cl	Au-OH	Au-Cl Stretch	Au-OH Stretch [4]	Au-Cl Stretch	Au-OH Stretch
$[AuCl_4]^-$	D_{4h}	A_{1g}, B_{1g}, B_{2g}	A_{1g}, B_{2g}		353 323		347 324 [4]		348 325	
$[AuCl_3(OH)]^-$	C_{2v}	$4A_1$, $3B_1$, $2B_2$	$2A_1$, B_1	A_1	352 341 324	624	339 [4]	569	348 335 325	566
$[AuCl_2(OH)_2]^-$ *cis*	C_{2v}	$4A_1$, A_2, $3B_1$, B_2	A_1, B_2	A_1, B_2	328 317	640 617			354 337	568 580
$[AuCl_2(OH)_2]^-$ *trans*	D_{2h}	$2A_g$, B_g,	A_g	A_g	343* 322*	623* 614*	356 [4]	576		
$[AuCl(OH)_3]^-$	C_{2v}	$4A_1$, $3B_1$, $2B_2$	A_1	$2A_1$, B_1	321	635 616 596	366 [4]	553	356	565 579 ?
$[Au(OH)_4]^-$	D_{4h}	A_{1g}, B_{1g}, B_{2g} (or $2A_{1g}$, $2B_{1g}$, $2B_{2g}$ E_g)		A_{1g}, B_{1g}				580		
$[AuCl_2]^-$ *(hydrated)*	$D_{\infty h}$	$\Sigma_g^+, \Sigma_u^+, \Pi_u$	Σ_g^+		269 *(273)*		329 [6] 332 [5]			
$[Au(OH)_2]^-$	$D_{\infty h}$	$\Sigma_g^+, \Sigma_u^+, \Pi_u$		Σ_g^+		533 502				
$[AuCl(OH)]^-$	$C_{\infty v}$	$2\Sigma^+, \Pi$	Σ^+	Σ^+	285	510	339 [5]			

Table 1: *Predicted numbers of Raman peaks, Raman frequencies, and experimental data for Au-chloro and chloro-hydroxy complexes. References: 1 Irish (1967); 2 Nakamoto (1986); 3 Tossell (1996); 4 Peck et al. (1991); 5 Pan and Wood (1991); 6 Braunstein and Clark (1973) (for $[AuCl_2]^-$ in crystalline salt) * : For these vibrations Tossell (1996) recorded vibrational modes without distinguishing which where Raman active. For both Au-Cl and Au-OH only one of the given frequencies is Raman active.*

Peck *et al.* (1991) therefore interpreted all their data in terms of hydrolysis of the Au(III) chloride complex. Pan and Wood (1991), however, suggested that these peaks could be assigned to Au(I) complexes. They stated that the $[AuCl_2]^-$ complex would be favoured over $[AuCl_4]^-$, not only with increasing temperature, but also with increasing pH or decreasing fO_2. They therefore suggested that a totally symmetric band at 336 Rcm^{-1} in the spectra of Peck *et al.* (1991) represented $[AuCl(OH)]^-$, but did not offer an explanation for the other bands in the Au-Cl region reported by Peck *et al.* (1991) at higher pH.

Farges *et al.* (1993) used EXAFS to study the local environment around Au(III) in aqueous 1M NaCl solutions at a range of pH values, and their results were consistent with the Raman data and interpretation of Peck *et al.* (1991). They found no evidence for Au(I) complexes, but stated that the results did not preclude the presence of minor amounts (less than 10%) of these complexes.

Published tables allow prediction of the number and polarisation of Raman and infrared active peaks in a spectrum, based on the molecular symmetry of the species. Calculations using bond lengths and force constants can predict the frequencies of these peaks, but the technique is complicated and by no means perfect. In addition, prediction of peak intensities is extremely difficult. Theoretical modelling of a number of gold complexes was conducted by Tossell (1996), who, amongst other factors, calculated vibrational frequencies for both Au(I) and Au(III) chloro- and hydroxy-complexes (Table 1). Although his frequencies matched the published experimental data reasonably well for the $[AuCl_4]^-$ complex, his predictions of Au-Cl stretching frequencies for mixed chloro-hydroxy Au(III) complexes did not agree with the data of Peck *et al.* (1991), and his predictions of Au-OH stretching frequencies were up to 50 Rcm^{-1} higher than the peaks observed by Peck *et al.* (1991).

Tossell (1996) stated that for each replacement step where one $(OH)^-$ ion is substituted for a Cl^- in the original $[AuCl_4]^-$ structure, the average Au-Cl stretching frequency would decrease by a few wavenumbers. He described the irregular upwards shifts of Peck *et al.* (1991) as "apparently unsystematic" but stated that it is possible that, as the relative peak intensities are unknown, other predicted peaks might be undetected in the spectra of Peck *et al.* (1991) due to low intensities. Although it is difficult to calculate the exact frequencies of bond vibrations, the trends in frequencies ought to be valid.

There is therefore disagreement over the interpretation of the data of Peck *et al.* (1991), as to whether the spectra obtained represent Au(I) or Au(III) complexes. There is also disagreement between the experimentally observed peak positions, and the number and frequency of the Raman peaks predicted theoretically. The purpose of this study therefore is to re-evaluate the speciation of gold-chloride complexes with pH, in order to resolve the discrepancies.

EXPERIMENTAL PROCEDURE

Raman analyses were carried out using a Jobin-Yvon T-64000 instrument in single spectrograph mode, using a single holographic grating of 1800g/mm together with a holographic notch filter to reject the laser light and an entrance slit of 50mm giving a resolution (defined as the full width at half maximum height of the 546.07nm line of a mercury lamp) of <2 Rcm^{-1}. Spectra were recorded using a liquid nitrogen cooled Spectrum One CCD detector. The precision of this set-up is better than $\pm$ 0.1 Rcm^{-1} for well-defined peaks. The 514.5nm line of a Coherent Innova 308 argon ion laser was used with a power at the sample of 50mW or less. An interference filter was used to remove laser plasma lines, but this was removed regularly during the analyses, and positions of the plasma lines checked. As the plasma lines occur within the range studied (520.3 and 266.3 Rcm^{-1}) this allowed an excellent control on the wavelength calibration. The samples were held in tubes and analysed in macro mode using a backscattering arrangement. In normal analyses no polarisation was applied to the scattered light, but several solutions were tested using both parallel and perpendicular polarisation to determine the depolarisation of the peaks. Analysis times varied depending on concentration, with longer count times being required for lower concentrations and higher pH values. Typically two spectra acquired for 2-5 minutes were averaged. Plating out of gold, due to photo-decomposition of the sample after long analysis times (Peck *et al.*, 1991), was not observed.

A number of solutions were prepared using varying concentrations of gold and total chloride, either as NaCl or HCl. The solution was prepared by dissolving hydrated tetrachloroauric acid ($HAuCl_4 \cdot 4H_2O$) in de-ionised water. In the first set of solutions, the salt was dissolved simply in the water. In a second set, minor excess chloride was added in the form of HCl, and in a third set significant excess chloride was added as 0.5M NaCl.

The pH was adjusted by the addition of small quantities of 1M NaOH or 0.7M HCl until the required pH was reached. A single solution was repeatedly adjusted and re-analysed The amounts of NaOH or HCl solution added were typically <0.1ml in 10ml of solution for each adjustment. At the end of the adjustment up to 1ml total may have been added, creating an overall dilution of <10%. Repeats were made at early and late stages of the dilution and adjustment process, and no systematic variation in the spectra was observed, indicating that this dilution had no significant effect on the speciation.

After pH adjustment, the pH was measured using a pH meter and solutions were analysed within a few minutes of preparation. Usually an immediate change in colour could be seen on adding acid or alkali: low pH solutions had a strong yellow colouration, which faded with increasing pH until solutions at high pH were colourless. This immediate change was taken to indicate that prolonged equilibration times were not necessary. This was supported by the fact that the spectra at a given pH were reproducible regardless of whether the solution had previously been at higher or lower pH.

When considering changes in the spectra, a number of different variables must be considered. The spectra of Pan and Wood (1991) and Peck *et al.* (1991) were discussed mainly in terms of the peak positions of Au-Cl stretches in the 320-360 Rcm^{-1} range, with some discussion of Au-OH stretches in the range 550-580 Rcm^{-1} in the latter paper. Peak fitting is essential in order to determine not just the positions but also the peak widths and relative intensities, measured as the integrated area under the peak. The intensity of the peaks relative to each other and other spectral features can give important information as to the relative abundances of the species under consideration.

For each spectrum, a number of parameters were determined. Peaks were fitted to the data in the Au-Cl stretching region, with a commercial statistical package (MicroCal Origin 4.1) using a least-squares fitting method. A Lorentzian function was found to give a better fit than a Gaussian, and provided the central peak position, the full width at half-maximum height ("width"), integrated area ("intensity") and height for each peak. The areas underneath the entire Au-Cl stretch region (300-380 Rcm^{-1}) and the Au-OH region (520-640 Rcm^{-1}) were also calculated to give an estimate of the relative intensities of all the peaks in each region, and therefore of the relative abundance of Au-Cl and Au-OH bonds. The relationship between these areas and the number of Au-Cl or Au-OH bonds is not a simple one, but it can be used as a first approximation. Although the intensity of a peak is proportional to the concentration of the species giving rise to that peak, a direct comparison of concentrations is not usually possible. For example, as noted by Pan and Wood (1991), the Au-Cl stretching peaks are likely to be more intense in $[AuCl_4]^-$, which contains four Au-Cl bonds, than in $[AuCl_3(OH)]^-$, which contains only three. In addition, Au-OH bonds will give peaks of different intensities to Au-Cl bonds, but broadly speaking, as the proportion of Au-OH bonds increases so too will the area ratio $A_{(Au\text{-}OH)}$ to $A_{(Au\text{-}Cl)}$.

RESULTS

Effect of Gold Concentration (in the Absence of Excess Chloride)

In the first set of solutions $HAuCl_4 \cdot 4H_2O$ was dissolved directly in de-ionised water, with no other added components. In these solutions total molar chloride concentration was therefore

exactly four times the total molar gold concentration. The resulting spectra for the Au-Cl stretching region are shown in Fig.17. At concentrations above 0.01M, the peaks representative of $[AuCl_4]^-$ are clear (348 and 325 Rcm^{-1}). At 0.01M, a third peak appears at 333 Rcm^{-1}, and is still present at 0.005M. At 0.001M, the signal is much weaker but two peaks can be discerned, at 350 and 333 Rcm^{-1}. The $[AuCl_4]^-$ peaks at 348 and 325 are no longer present. The pH range covered in these solutions is from 1.7 (0.04M) to 3.2 (0.001M).

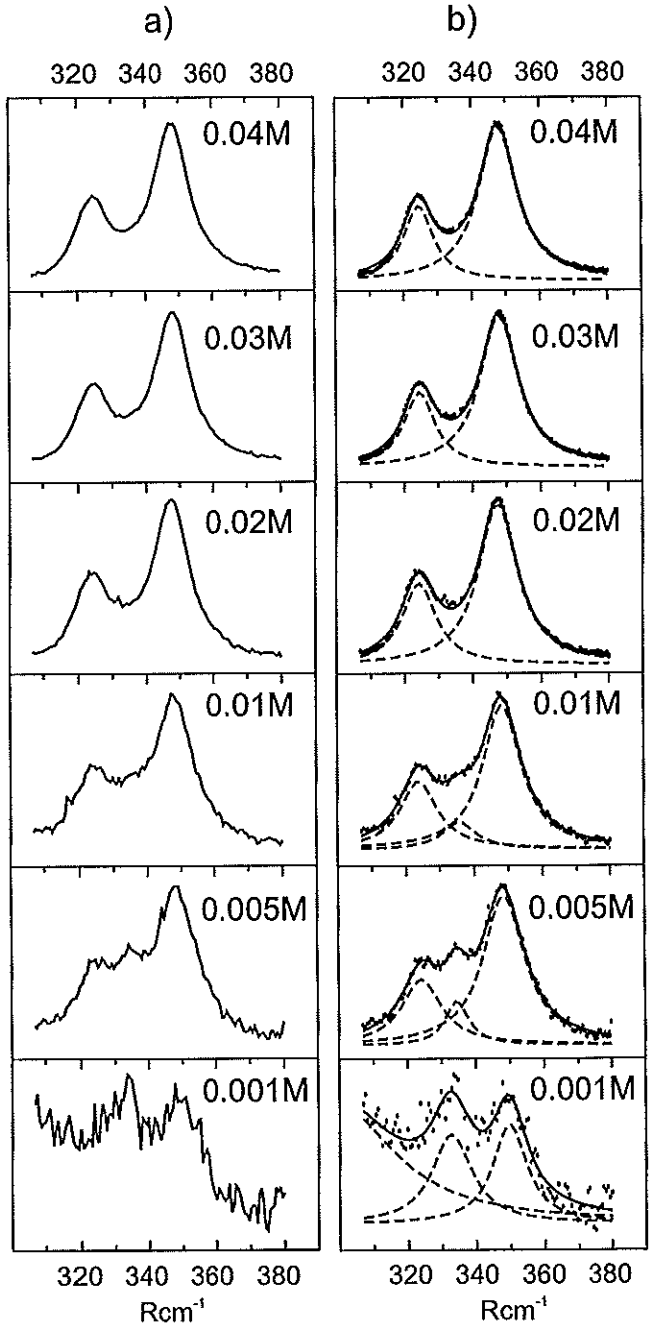

Figure 17. Effect of concentration on Raman peaks in the Au-Cl stretching region, for solutions in the absence of excess chloride. Intensity is not necessarily to scale. a)Original data b) Dotted lines = fitted Lorentzian peaks; solid lines = sum of fitted peaks; dots = original data

It is apparent from these spectra that in the absence of excess chloride ($\Sigma Cl/\Sigma Au = 4$) and at low gold concentrations, the $[AuCl_4]^-$ complex is less stable, and is replaced by another, probably chloride-depleted complex. The peak assignments and discussion of the complexes formed will be covered in a later section.

The observation that dilute solutions in the absence of excess chloride are likely to be dominated by hydrolysed complexes is interesting but is unlikely to be of much importance in geological systems, since natural solutions can generally be assumed to contain excess chloride relative to gold.

Effect of Chloride Concentration

The effect of chloride concentration was studied in very dilute solutions, by analysing several solutions of identical gold concentration (0.001M) but varying chloride concentrations. The resulting spectra are very weak (Fig.18) but clear differences are seen between solutions with minor or substantial excess chloride. As described above, the 0.001M solution with no excess chloride showed very weak peaks at 350 and 333 Rcm^{-1} (Fig. 18a). The addition of very minor excess chloride in the form of HCl, (to give pH ≈3) resulted in extremely weak peaks representative of $[AuCl_4]^-$ (Fig.18b). The addition of substantial excess chloride either as NaCl (having negligible effect on pH) increased the peak intensity (Fig 18c). Addition of major excess chloride as HCl (decreasing the pH to <2) resulted in much stronger spectra typical of the $[AuCl_4]^-$ complex (325 and 348 Rcm^{-1}; Fig.18d). Although the effect of adding chloride while reducing pH is the most pronounced, the effect of excess chloride with no change in pH, is also significant.

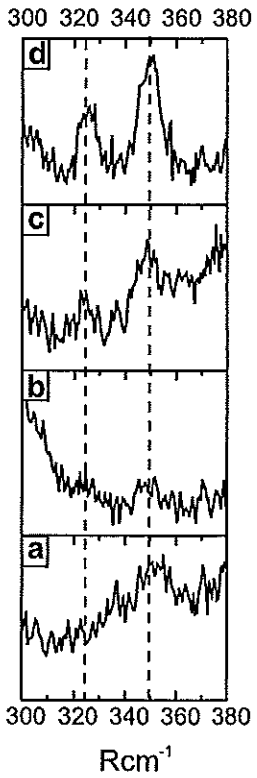

Figure 18. Effect of the addition of chloride to low concentration solutions. Intensity is not necessarily to scale. a)0.001M, no excess chloride b)0.001M + minor Cl as HCl c)0.001M + chloride as 0.5M NaCl d) 0.001M + chloride as 0.75M HCl

Spectra 2(b)-(d) were obtained under identical conditions. Under the same conditions, no peaks were obtained for the solution in the absence of excess chloride, and with a longer count time, the signal was still very weak (Fig. 18a). It is clear from Fig 18(d) that it is possible to obtain reasonable spectra at this low gold. The problem in obtaining a signal therefore appears to be due to the concentration of $[AuCl_4]^-$ rather than the concentration of gold, and the weakness of spectra (a) and (b), and to a lesser extent (c) is due to the partial or complete transformation of $[AuCl_4]^-$ to another complex, having a weaker Raman signal.

Effect of Varying pH

The effect of pH on the Raman spectra was studied by adjusting the pH and repeatedly re-analysing a single solution. The various features of the changes seen in the spectra of a single solution will be discussed with regard to one solution (a 0.02M $HAuCl_4 \cdot 4H_2O$ + H_2O solution containing very minor excess chloride) and then other solutions compared to this one.

The spectra for this solution are presented in Figure 19. At pH 1.68, the spectrum consists of two peaks, at 325 and 348 Rcm^{-1}, which represent Au-Cl stretches. No peaks are present in the region around 580, where Peck *et al.* (1991) described Au-OH stretches. The Au-Cl in-plane bending peak at 171 Rcm^{-1} (as described by Pan and Wood (1991) is relatively low and broad, and except at high concentrations is often obscured by a water-related peak at 210 Rcm^{-1}. It will therefore not be discussed further in this paper.

Peaks in the AuCl stretching region were fitted as before, and the variation in the parameters obtained is shown in Fig. 20. At low pH two main peaks are present: 348 Rcm^{-1} (assigned to the totally symmetric Au-Cl stretch; polarisation features indicate it is totally symmetric) and 325 Rcm^{-1} (asymmetric Au-Cl stretch). These peaks are consistent with previously published data for the $[AuCl_4]^-$ complex, both experimentally (Pan and Wood, 1991; Peck *et al.*, 1991) and theoretically (Tossell, 1996).

Looking at the graphs of data for the 0.02M solution (Fig.20), the data can be divided into 5 pH ranges showing different characteristics:

a) pH < 4 Two peaks are present: 348 and 325 Rcm^{-1} ($[AuCl_4]^-$) The solution is yellow in colour.

b) pH 4-5 Three peaks are present: the two earlier peaks still remain, and there is a new peak at 335 Rcm^{-1}, which grows in size. All three have consistent peak positions but variable widths. The solution is a very light yellow colour.

c) pH 5.5-6.5 Two peaks are present: the 335 moves gradually to 337 Rcm^{-1} and a new peak appears at 353-354 Rcm^{-1} and moves to 356 Rcm^{-1}. The peaks at 348/325 are no longer present. The solution is colourless.

d) pH 6.5-9 The 356 peak becomes dominant over the 337 peak (which also shifts in frequency towards 340 Rcm^{-1}), and becomes much wider.

e) pH > 9 Only the 356 peak is present. There is little clear change in position or peak width. At pH>10 a dark violet precipitate appears, which redissolves when the pH is reduced, or when excess NaOH is added. This precipitate gave no Raman spectrum.

Variations in peak width may be due to the presence of two separate but unresolved peaks, resulting in a greater intensity and wider shape.

The quality of the spectra deteriorate rapidly above pH 5: the spectra shown at high pH were typically obtained with count times several times those at low pH, but even so they have very low signal:noise ratios. This reduced signal makes the determination of peak position and width calculations much more difficult: overlap of peaks is a problem with peak positions only a few wavenumbers apart, and half-height widths of 10 or more. Nonetheless, a consistent shift in peak position can be observed (Fig.20).

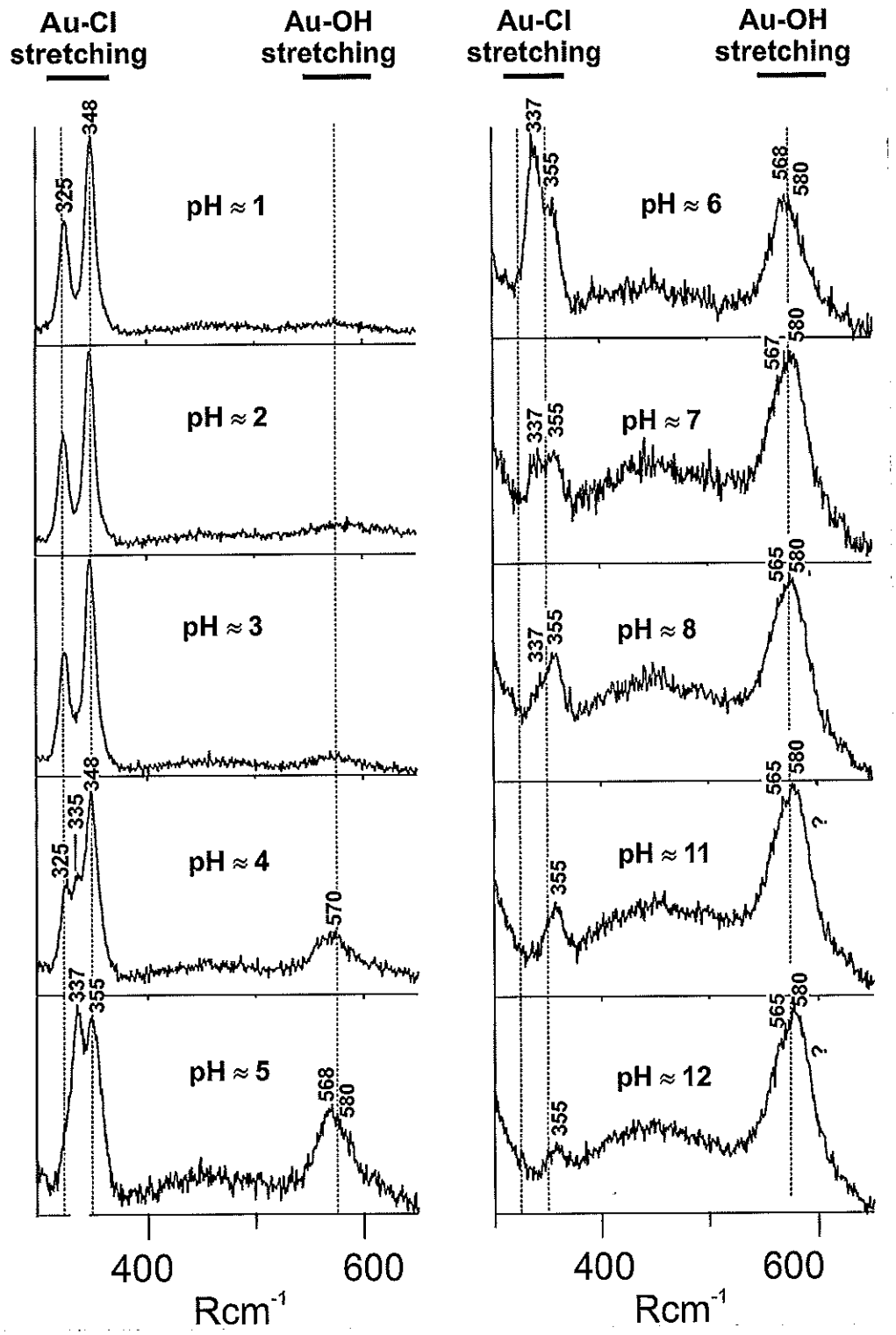

Figure 19. Representative Raman spectra showing the effect of pH for 0.02M $HAuCl_4 4H_2O$ solution, for both Au-Cl stretching and Au-OH stretching ranges. Vertical lines are shown for comparison of peak positions. Intensity is not necessarily to scale. The feature that is cut off at the low frequency range for high pH values is due to water, and was also present , but relatively insignificant, at lower pH values.

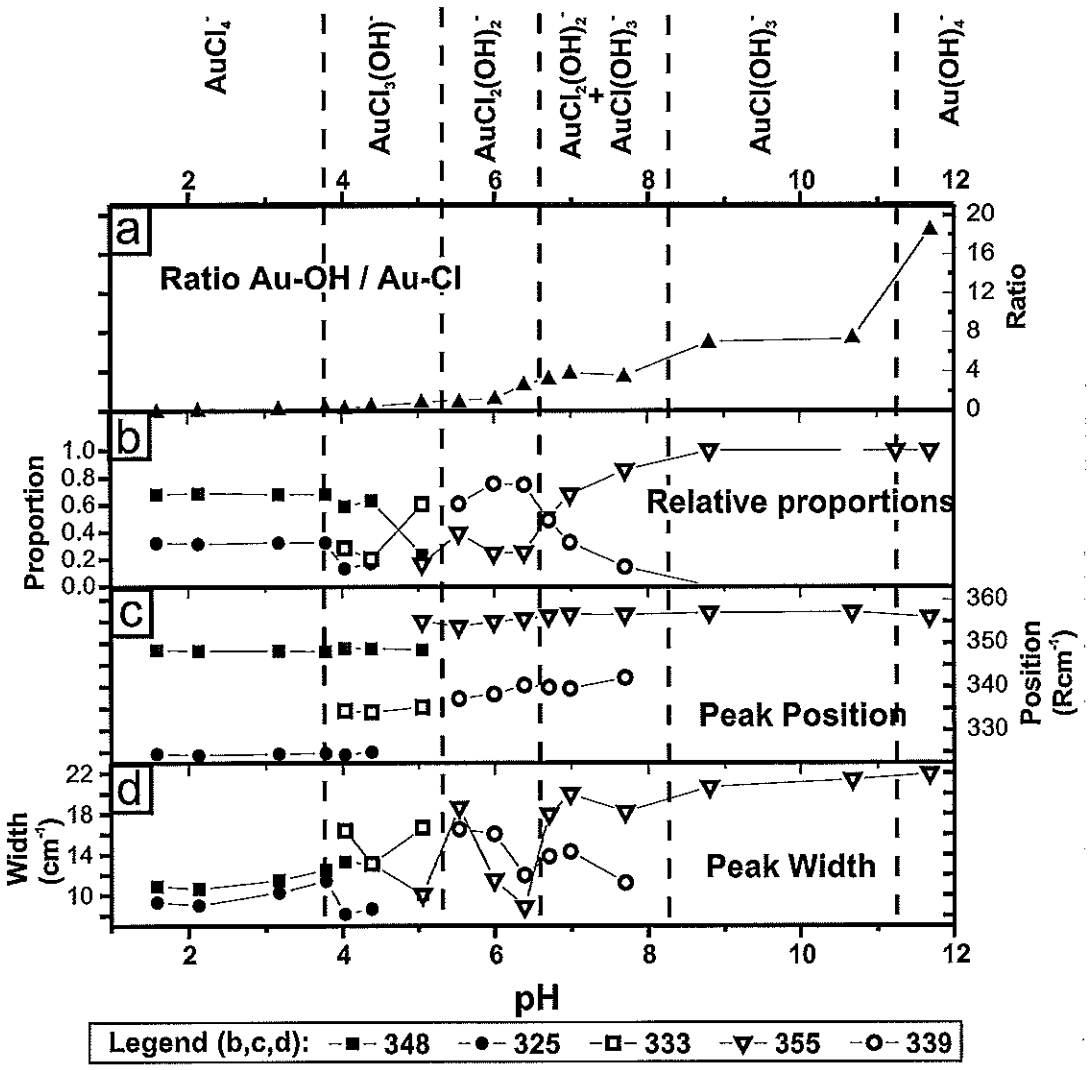

Figure 20. Variation in the parameters calculated from peak fitting for 0.02M solution over a range of pH, together with assigned complex ion species. a) Ratio of integrated areas under the Au-Cl stretching region (300-380 Rcm^{-1}) and Au-OH stretching region (520-640 Rcm^{-1}) b) Relative proportions of peaks (i.e. area of peak as a proportion of the total area of all peaks) c) Peak positions d) Full width at half maximum height.

The 352-355 Rcm^{-1} peaks show the same polarisation characteristics as the original 348 Rcm^{-1} peak, suggesting that they are also totally symmetric Au-Cl stretches. The peak at 335Rcm^{-1} is also polarised, but to a lesser degree, and they are also likely to represent symmetrical stretches. However, the 337Rcm^{-1} peak in the neutral pH range is not polarised, indicating that it is not totally symmetric.

Peaks representing Au-OH stretches occur in the region around 580 Rcm^{-1} and are not as clearly resolved as those in the Au-Cl stretching region. The band is usually asymmetric, but it is not possible to distinguish individual peaks: it may be that numerous Au-OH peaks are present, all overlapping, or simply two peaks that are wider than the Au-Cl bands and therefore impossible to resolve individually.

Au-OH stretching peaks become visible by pH = 3.17 but strong by 3.78 (Fig. 19). At pH ≈4 a single peak appears to be present at around 570 Rcm^{-1}. By pH=5, two peaks are present at ≈568 and 580 Rcm^{-1}. Between pH 6 and 7, a major change occurs with the band becoming skewed to high frequencies, and although no peaks are clearly visible at least two must be present to cause the asymmetric shape. This asymmetry becomes more pronounced as the pH is

increased, although no further major changes in the band shape are observed. The shape of the band suggest it is made up of two or probably three peaks, but it is not possible to clearly identify the positions of intensities of these peaks. There is however an increase in the average frequency (and in particular the frequency of the band maximum) as the pH is increased.

The ratio of Au-Cl stretch to Au-OH stretch areas is shown in Figure 20(a). Several pH ranges show relatively rapid growth of the Au-OH region to relative to the Au-Cl stretches. These are likely to represent transitions from one complex to another, and are within the regions: pH 5.5-6.5, 8-9, and 11-12. Growth is also observed between pH 4 and 5, but at a much slower rate.

Effect of Concentration on pH of Hydrolysis

The experiment as described above was repeated for a number of similar solutions of different concentration. Solutions analysed for the effect of pH were as follows:

a) 0.005M $HAuCl_4 \cdot 4H_2O$ in H_2O
b) 0.01M $HAuCl_4 \cdot 4H_2O$ in H_2O
c) 0.01M $HAuCl_4 \cdot 4H_2O$ in 0.5M NaCl

Each solution was adjusted to the required pH using NaOH and HCl

The parameters of the peaks were obtained in the same way as for the 0.02M solution, and the data show essentially similar features. However, the pH values at which the different peaks occur are rather different (Fig. 21). Duplicate solutions were prepared and the pH values of the transitions were found to be consistent. The results show that at lower concentrations the pH values at which the transitions between complexes take place are reduced, allowing hydrolysis at lower pH. Such an observation has important implications, as all the solutions in this study are by necessity several orders of magnitude more concentrated than natural gold-bearing solutions.

For solutions in the absence of excess chloride no pH adjustments were carried out, but the peaks observed at low concentrations for 0.005M and 0.001M are similar to those recorded at pH $\approx$ 5 and 8 respectively for the 0.02M solution.

Effect of Major Excess Chloride on pH of Hydrolysis

Two solutions were prepared with identical gold concentration but different total chloride contents, and the effect of pH on the speciation in these solutions was studied. The first solution contained 0.01M Au with very minor excess chloride from HCl, while the second was in 0.5M NaCl. The results (Fig. 21) show that the pH ranges for peak appearances are shifted to higher values with additional chloride, indicating that excess chloride reduces hydrolysis.

DISCUSSION

When predicting the number of Raman peaks in a spectrum, it is necessary to know the symmetry of the molecule. In this study the symmetry groups used to define the complexes assume free rotation of the –OH groups (treating them as single ligands), and the Au-OH stretches referred to throughout this paper are in fact Au-O(H) stretches. In practice, the Au-O-H bonds are likely to form a bend reducing the overall symmetry of the molecule, but the central unit ($Au\ Cl_x\ (O)_{4-x}$) can be treated as a single square planar form without considering the O-H bonds, as the space group symmetry of the central Au atom remains the same. Similarly, O-H and Au-O-H bond vibrations will cause additional Raman lines in the spectrum, but the O-H stretching and Au-O-H bending are likely to be swamped by the far more intense O-H stretch and H-O-H stretching and bending modes due to water. These modes are therefore not discussed further in this study.

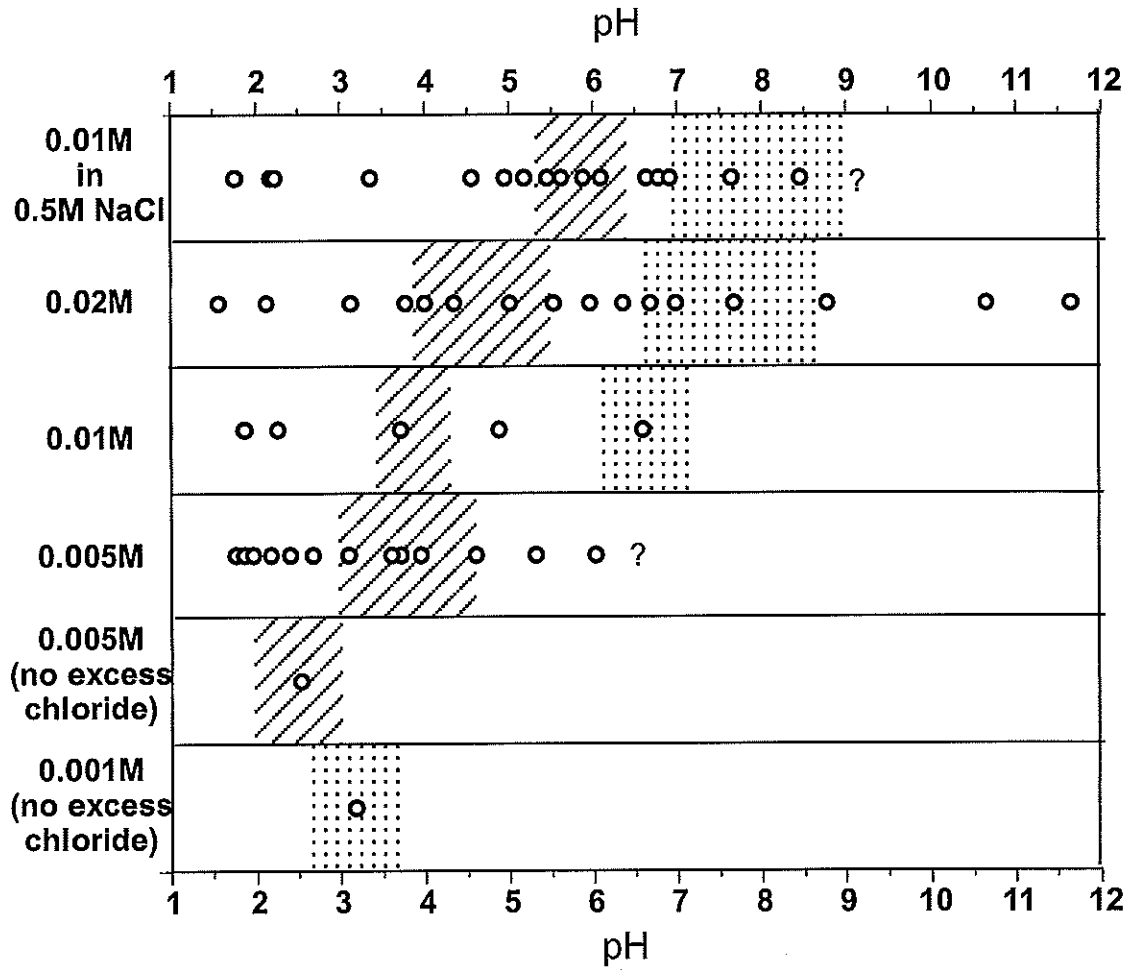

Figure 21. Effect of concentration on complex speciation: changes in the pH of complex dominance boundaries calculated from plots of relative peak proportions. pH values for analyses are marked. Hashed area: 348,335 and 325 Rcm^{-1} peaks [$(AuCl_3(OH)]^-$ complex. Dotted area: 337 and 355 Rcm^{-1} peaks (355 increasingly dominant) with $[AuCl_2(OH)_2]^-$ and $AuCl(OH)_3]^-$ complexes coexisting. The uncertainty of transitions varies for the different solutions depending on the number of data points.

Assignment of Peaks

If increasing pH results in the expected Au(III) hydrolysis sequence $[AuCl_x(OH)_{4-x}]^-$ then each change in the Raman spectra should represent a transition where one [Cl]- is replaced by one [OH]-.

Table 1 shows the number of bands predicted by theoretical studies for each species, along with experimental data from previous workers. The number of peaks expected to occur in the Raman spectrum for each complex is determined simply, by reference to the symmetry of the molecule and published tables (e.g. Irish, 1967; Nakamoto, 1986), while the frequencies are predicted by much more sophisticated methods involving bond lengths, force constants, etc. Comparison of the results of this study with the theory for the hydrolysis sequence $[AuCl_x(OH)_{4-x}]^-$ shows the following (Table 1):

For $[AuCl_4]^-$ two Au-Cl stretches are expected, which is consistent with the observed spectrum at pH<4 with peaks at 325 and 348 Rcm^{-1}. These frequencies are also consistent with data from previous workers (Pan and Wood, 1991; Peck *et al.*, 1991) and are in close agreement with the predictions of Tossell (1996).

For $[AuCl_3(OH)]^-$ three Au-Cl stretches and one Au-OH stretch are expected in the Raman spectrum. In this study, at pH values from 4 to 5, three Au-Cl stretching bands are observed, at

325, 335 and 348 Rcm^{-1}. Two of these are identical to those for the $[AuCl_4]^-$ complex, but much weaker. A single band in the Au-OH stretching region is also observed. It is possible that the 348 and 325 Rcm^{-1} peaks still represent the $[AuCl_4]^-$ complex, and only the 335 peak is due to a new complex. However, a number of other factors suggest that all three peaks are due to the new complex. Between pH 3 and 4 the signal/noise ratio decreases, (Fig. 19), and this coincides with the appearance of the 335 peak. At this point there is a slight increase in the width of the 348 peak and a more pronounced decrease in the width of the 325 peak. Although these changes are small, their occurrence at the same point as the introduction of the third peak suggests that they are significant. In addition, the 335 Rcm^{-1} peak is never observed in the absence of the other two, suggesting that they represent a single complex. These spectra are consistent with the prediction of Tossell (1996) for the $[AuCl_3(OH)]^-$ complex of two peaks very close to those of $[AuCl_4]^-$, and a third peak between them (Table 1).

The complex $[AuCl_2(OH)_2]^-$ may occur as either the *cis* or *trans* form. The *cis* form should show two each of Au-OH and Au-Cl stretches (of which only one is polarised) while the *trans* form would be expected to show only one of each. For pH values of 5 to 6.5, two bands are present in the Au-Cl stretching region, at 337 and 355 Rcm^{-1}. Only one of these (355 Rcm^{-1}) is polarised. The Au-OH region also shows two peaks. These spectra are therefore consistent with the presence of the *cis* form of $[AuCl_2(OH)_2]^-$. By contrast, Peck *et al* (1991) suggested the presence of the *trans* form, based on their identification of only one Au-Cl peak.

The $[AuCl(OH)_3]^-$ can be considered as the inverse of $[AuCl_3(OH)]^-$, showing three Au-OH stretches and one Au-Cl. At pH values above 6.5, the 337 Rcm^{-1} peak reduces rapidly and the 356 Rcm^{-1}peak is the only one remaining. The Au-OH region shows at least two peaks, although the individual peaks cannot be discerned and it is possible that three peaks are present.

The $[Au(OH)_4]^-$ species would be expected to show two Au-OH stretches. Although all the solutions analysed produced weak bands in the Au-Cl region, indicating the presence of at least minor chloride-bearing species, the jump in Au-OH/Au-Cl ratio at pH>11 suggests the formation of $[Au(OH)_4]^-$ alongside $[AuCl(OH)_3]^-$. The Au-OH peaks are much weaker than those for Au-Cl: at very high pH they do not reach the same intensity as the Au-Cl peaks at low pH. This shows that a simple intensity comparison between the peaks is not directly representative of concentration.

The sequence of peaks observed in this study is therefore consistent with the Au(III) hydrolysis sequence $[AuCl_x(OH)_{4-x}]^-$. There is no evidence for the formation of Au(I) complexes as suggested by Pan and Wood, (1991). The frequencies predicted by Tossell (1996) for Au(I) complexes (Table 1) are much lower than those observed here, although Pan and Wood, (1991) assigned their observed peak at 332 Rcm-1 to the Au-Cl stretch in $[AuCl_2]^-$. More importantly, only one Au-Cl stretch should be present for $[AuCl_2]^-$ and $[AuCl(OH)]^-$ whereas in this study more than one Au-Cl peak was present at all times. Similarly, the $[AuCl(OH)]^-$ complex should show only one Au-OH stretching peak, while at most pH values two were observed. The $[Au(OH)_2]^-$ would show no Au-Cl peaks. We can therefore conclude that under all conditions studied here gold was present as Au(III) chloride and mixed chloro-hydroxy complexes, and that Au(I) complexes were not present in significant amounts.

Contrast with Previous Work

The results presented here differ from those of Peck *et al.* (1991) in a number of ways (Fig.22). Although the peak positions recorded are similar, in this study the Au-Cl peaks occur as groups of two or three for each complex; the polarisation characteristics of the peaks are different; the pH range for each complex is different, with hydrolysis reactions beginning at

considerably lower pH in this study; and the precipitate formed at high pH is different in the two studies.

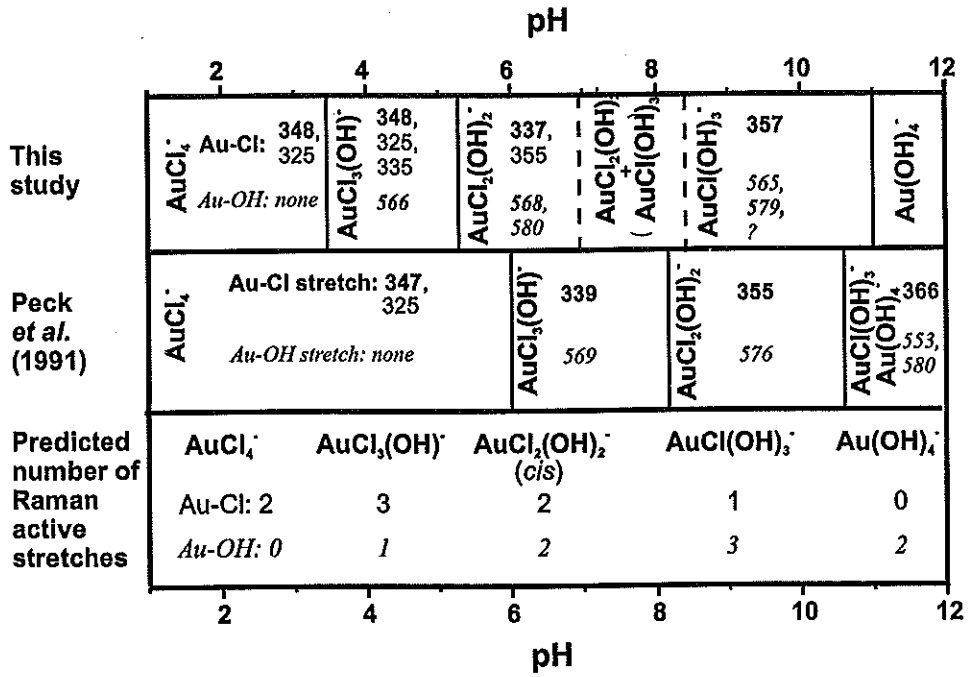

Figure 22. Comparison of the assigned Raman stretching frequencies and pH ranges of dominance for the $[AuCl_x(OH)_{4-x}]^-$ sequence of complexes, compared to the data of Peck et al.(1991), and the number of Raman peaks predicted theoretically.

At most pH values in this study more than one Au-Cl stretching band is present, while in the spectra of Peck *et al.* (1991) peaks were found to occur singly for pH values above six. In the present study peak resolution was improved and peak-fitting techniques allowed a better determination of the peaks present at each stage. The numbers of peaks present for each step in this study are consistent with theory for the Au(III) hydrolysis sequence. The peaks observed by Peck *et al.* (1991) suggest a simpler complex. Although other peaks might be present but unobserved due to low intensities (Tossell, 1996) the comparison between spectra from the two studies suggests that this is unlikely. In addition, the peak at 337 Rcm^{-1} observed in this study is non-totally symmetric, while that reported by Peck *et al.* (1991) at the same position was totally symmetric. In the latter case, a simple linear Au(I) form is more likely.

In the data of Peck *et al.* (1991) hydrolysis of the $[AuCl_4]^-$ complex was first recognised at a pH ≈5.8. In this study, changes in the spectra are first recorded at pH=3.8, and each subsequent hydrolysis step occurs 2-3 pH units lower than described by Peck *et al.* (1991). Such a change is extremely significant, since pH values less than four are common in hydrothermal fluids suggesting that hydrolysis reactions may be important in chloride-bearing hydrothermal fluids as well as in surface waters.

The different colours of the precipitates formed at high pH in this study and in that of Peck *et al.* (1991) serve to illustrate the different speciation that must be present in the two studies. A number of oxides and hydroxides are known, of both Au(I) and Au(III). In general, Au(III) forms yellow or brown oxides and hydroxides, whereas Au(I) forms violet solids (Laist, 1954). Solid chlorides are generally yellow or red in colour and are unlikely to form in this situation. The precipitate formed in this study was a dark purple-grey colour, and is likely to be gold (I)

hydroxide, which has been described as a dark violet solid forming on addition of KOH to a gold (I) chloride solution (Laist, 1954). The occurrence of Au(I) hydroxide does not necessarily indicate the presence of Au(I) in solution. The precipitation is likely to have been caused by the reduction of Au(III) in solution. By contrast, the precipitate described by Peck *et al.* (1991) was white and was assumed to be a hydroxide. However, Laist (1954) describes no white hydroxides or oxides of gold, and the correct identification of this precipitate is not clear.

It is clear both from the Raman spectra and the precipitate at high pH that the speciation in the solutions of this study and that of Peck *et al.* (1991) are different. The factors discussed above suggest that in the present study gold was present as Au(III) chloro-hydroxy complexes, but that the spectra of Peck *et al.* (1991) represent different complexes, probably of Au(I).

The conditions for this study and that of Peck *et al.* (1991) were very similar, except for concentrations and equilibration time. The solutions of Peck *et al.* (1991) were much more concentrated both in terms of gold (0.1M Au compared to 0.04-0.001M in this study) and chloride (1M NaCl compared to <0.1M ΣCl in this study). Lower chloride concentrations would normally be expected to make Au(I) complexes more, not less, likely in the latter case.

Peck *et al.* (1991) allowed their solutions to equilibrate for several hours after pH adjustment before Raman analysis. In this study, the delay was generally 10 minutes or less. However, the reproducibility of results in this study when approaching a pH value from either above or below indicated no problem with equilibration.

Pan and Wood (1991) describe differences of 4-7 Rcm^{-1} as at the limit of the margin of error for Raman measurements/peak positions, but we disagree with that assumption. All workers agree on the positions of the accepted $[AuCl_4]^-$ Au-Cl stretches to within $\pm$ 1 Rcm^{-1} of 348 and 325 Rcm^{-1}. Where a single peak is present, as in the spectra of Peck *et al* (1991) or where peak fitting methods are used as in this study and that of Pan and Wood (1991) the frequencies of other peaks should be recorded with a similar degree of accuracy. Although the intensity of the peaks for other complexes may be lower, and the overlap with other peaks causes some interference, the accuracy is unlikely to be reduced to 5 Rcm^{-1}, except where the spectra are very weak (e.g., at very high pH or at very low concentrations). It is more likely that the peaks involved are in fact different in at least some cases.

Contrast with Theoretical Predictions

Tossell (1996) suggests that $[AuCl(OH)]^-$ is not present in the spectra of Peck *et al.* (1991), as he predicts the Au-Cl stretch in this complex to occur $15cm^{-1}$ above than that in $[AuCl_2]^-$, and also that the Au-OH stretch would occur more than $100cm^{-1}$ below that in $[AuCl_3(OH)]^-$. However, he admits that the errors in the theoretical calculations vary in Au(I) and Au(III) species. In $[AuCl_4]^-$, his predicted Au-Cl stretches agree closely with experimental values, whereas those in $[AuCl_2]^-$ are much lower than reported experimental values (Table 1).

Tossell (1996) also predicts that the average frequency of the Au-Cl stretches should decrease by a few wave numbers for each successive step of replacement of Cl^- by $[OH]^-$. Although the values from this study for $[AuCl_4]^-$ and $[AuCl_3(OH)]^-$ agree closely with the predictions, the peaks of more chloride-depleted complexes move to higher frequencies, both in this study and in that of Peck *et al.* (1991).

For peaks in the Au-OH stretching region, Tossell, (1996) predicts that the peak frequencies should increase with increasing –OH substitution, and this is observed both in this study and in that of Peck *et al.* (1991). However, both sets of experimental values are some $50cm^{-1}$ lower than the predicted frequencies, suggesting a problem in the theoretical frequency calculations.

CONCLUSIONS

Pan and Wood (1991) described minimum concentrations for Raman spectroscopy of 0.1 to 0.01M, and Peck *et al.* (1991) used 0.1M Au solutions, compared to gold concentrations in hydrothermal fluids of the order of 10^{-9}M (Seward, 1991). The solutions used in this study were up to an order of magnitude more dilute than those used in previous studies, showing that with modern instrumentation Raman spectroscopy can be applied to solutions closer to geologically realistic conditions of concentration compared to earlier studies. In the presence of excess chloride $[AuCl_4]^-$ could easily be detected in 0.001M solutions.

By comparison with the data of Peck *et al.* (1991) the spectra produced in this study have improved resolution allowing clearer determination of peak positions. The spectra produced are more consistent with theoretical predictions and show that, under these conditions hydrolysis of the $[AuCl_4]^-$ complex occurs at much lower pH than previously found or predicted. At low total gold and chloride concentrations no evidence was found for Au(I) complexes across a pH range of 1-11. In the light of these data, the spectra of Peck *et al.* (1991) do not appear to represent the same group of species. Peck *et al.* (1991) were probably dealing with Au(I) complexes over some of their pH range and the difference is likely to be due to their much higher chloride contents than in this study. The reason for the difference between the two sets of data is something that requires further study.

Concentration both of gold and total chloride was found to have a significant effect on the pH ranges of stability for the various chloro-hydroxo species. The higher the gold concentration, the higher the pH of hydrolysis. Similarly, the higher the total chloride concentration, the higher the pH values of hydrolysis.

These results indicate that Au(III) chloro-hydroxy species may be important over a wider range of fluid conditions than previously thought. Au(III) chloride complexes may be hydrolysed, not only in surface waters but also under pH conditions common on hydrothermal fluids. The effect of pH at high temperature must now be studied in order to determine the how important such hydrolysis reactions might be in hydrothermal fluids.

_____oOo_____

REFERENCES

Benning L. G. and Seward T. M. (1996) Hydrosulphide complexing of Au(I) in hydrothermal solutions from 150-400°C and 500-1500 bar. *Geochimica et Cosmochimica Acta* **60**, 1849-1871.

Braunstein P. and Clark R. J. H. (1973) The preparation, properties and vibrational spectra of complexes containing the $AuCl_2^-$, $AuBr_2^-$ and AuI_2^- ions. *J. Chem. Soc.*, 1845-1848.

Burke E. A. J. (1994) Raman microspectrometry of fluid inclusions: the daily practice. In *Fluid inclusions in Minerals: methods and applications (IMA '94 Short Course, Siena)* (ed. B. de Vivo and M. L. Frezzotti), pp. 25-44. Virginia Tech.

Catledge S. A., Vohra Y. K., Ladi R., and Ral G. (1996) Micro-Raman stress investigations and X-ray diffraction analysis of polycrystalline diamond (PCD) tools. *Diamond and Related Materials* **5**, 1156-1165.

Chou I.-M., Pasteris J. D., and Seitz J. C. (1990) High-density volatiles in the system C-O-H-N for the calibration of a laser Raman microprobe. *Geochim. Cosmochim. Acta* **54**, 535-543.

Cotton F. A. and Wilkinson G. (1988) *Advanced Inorganic Chemistry*. John Wiley and Sons.

Daniel I., Gillet P., Poe B., and Mcmillan P. (1995) In-situ high-temperature Raman-spectroscopic studies of aluminosilicate liquids. *Physics and Chemistry of Minerals* **22**(2), 74-86.

Dao N., Quang V., Huy N., and Silvestre J. (1996) Discovery of diamond inclusions in rubies. *Comptes Rendus De l Academie des Sciences Paris* **322**(6,), 515-522.

de Faria D. L. A., Venanciao Silva S., and de Oliviera M. T. (1997) Raman microspectroscopy of some iron oxides and oxyhydroxides. *Journal of Raman Spectroscopy* **28**, 873-878.

Dhamelincourt P., Beny J. M., Dubessy J., and Poty B. (1979) Analyse d'inclusions fluides à la microsonde MOLE à effet Raman. *Bull. Minéral.* **102**, 600-610.

Dubessy J., Boiron M.-C., Moisette A., Monnin C., and Sretenskaya N. (1992) Determinations of water, hydrates and pH in fluid inclusions by micro-Raman spectrometry. *Eur. J. Min.* **4**, 885-894.

Dubessy J., Poty B., and Ramboz C. (1989) Advances in C-O-H-N-S Fluid Geochemistry based on Micro-Raman Spectrometric Analysis of Fluid Inclusions. *Eur.J.Mineral.* **1**, 517-534.

Fabre D. and Oksengorn B. (1992) Pressure and Density dependence of the CH_4 and N_2 Raman lines in an equimolar CH4/N2 gas mixture. *Applied Spectrscopy* **46**, 468-471.

Farges F., Sharps J. A., and Brown G. E. J. (1993) Local environment around gold (III) in aqueous chloride solutions: an EXAFS spectroscopy study. *Geochimica et Cosmochimica Acta* **57**, 1243-1252.

Gammons C. H. and Williams-Jones A. E. (1995a) Hydrothermal geochemistry of electrum: thermodynamic constraints. *Economic Geology* **90**, 420-432.

Gammons C. H. and Williams-Jones A. E. (1995b) The solubility of Au-Ag alloy + AgCl in HCl/NaCl solutions at 300°C: New data on the stability of Au(I) chloride complexes in hydrothermal fluids. *Geochimica et Cosmochimica Acta* **59**, 3453-3468.

Gammons C. H., Yu Y., and Williams-Jones A. E. (1997) The disproportionation of gold(I) chloride complexes at 25 to 200°C. *Geochimica et Cosmochimica Acta* **61**, 1971-1983.

Genge M., Jones A., and Price G. (1995) An infrared and Raman-study of carbonate glasses - implications for the structure of carbonatite magmas. *Geochimica et Cosmochimica Acta* **59**(5), 927-937.

Gillet P., Fiquet G., Malezieux J.M., and Geiger C.A. (1992) High-pressure and high-temperature Raman spectroscopy of end-member garnets; pyrope, grossular and andradite *European Journal of Mineralogy*, **4**, 651-664

Gillet, P. (1996) Raman spectroscopy at high pressure and high temperature. Phase transitions and thermodynamic properties of minerals *Phys. Chem. Minerals,* **23**, 263-275

Gillet, P., Fiquet, G., Daniel, I. And Reynard, B. (1993) Raman spectroscopy at mantle pressure and temperature conditions: experimental set-up and the example of CaTiO3 perovskite *geophysical Research Letters,* **20**, 1931-1934

Griffith W. P. (1975) Raman spectroscopy of terrestrial minerals. In *Infrared and Raman Spectroscopy of Lunar and Terrestrial Minerals* (ed. C. J. Karr), pp. 299-323. Academic Press.

Hayashi K. I. and Ohmoto H. (1991) Solubility of gold in NaCl- and H_2S-bearing aqueous solutions at 250-350°C. *Geochimica Cosmochimica Acta* **55**, 2111-2126.

Irish D. E. (1967) Raman spectroscopy of complex ions in solution. In *Raman spectroscopy: theory and practice* (ed. H. A. Szymanski), pp. 224-250. Plenum.

Kingma K., Cohen R., Hemley R., and Mao H. (1995) Transformation of stishovite to a denser phase at lower-mantle pressures. *Nature* **374**(6519), 243-245.

Laist J. W. (1954) Copper, Silver and Gold. In *Comprehensive Inorganic Chemistry*, Vol. II (ed. M. C. Sneed, J. L. Maynard, and R. C. Brasted), D Van Noshrand Co.

McCormick T. L., Jackson W. E., and Nemanich R. J. (1997) The characterization of strain, impurity content, and crush strength of synthetic diamond crystals. *Journal of Material Research* **12**(1), 253-263.

McMillan P. F. (1989) Raman Spectroscopy in Mineralogy and Geochemistry. *Ann.Rev.Earth Planet.Sci.* **17**, 255-283.

Mernagh T. P. (1991) Use of the laser Raman microprobe for discrimination amongst feldspar minerals. *Journal of Raman Spectroscopy* **22**, 453-457.

Mernagh T. P. and Trudu A. G. (1993) A laser Raman microprobe study of some geologically important sulphide minerals. *Chemical Geology* **103**, 113-127.

Mitsuhashi M., Karasawa S., Ohya S., and Togashi F. (1993) Relation between the dislocations in chemically vapour-deposited diamond and the linewidth of the Raman spectrum. *Thin Solid Films* **228**, 76-79.

Miyamoto M. and Ohsumi K. (1995) Micro-Raman-spectroscopy of olivines in l6 chondrites - evaluation of the degree of shock. *Geophysical Research Letters* **22**(4), 437-440.

Murphy P. J. and Roberts S. (1995) Laser Raman spectroscopy of differential partitioning in mixed-gas clathrates in H_2O-CO_2-N_2-CH_4 fluid inclusions: Implications for microthermometry. *Geochim. Cosmochim. Acta.* **59**(23), 4809-4824.

Murphy P. J. and Roberts S. (1997) Melting and nucleation behaviour of clathrates in multivolatile fluid inclusions: evidence of thermodynamic disequilibrium. *Chemical Geology* **135**, 1-20.

Mycroft J. R., Bancroft G. M., McIntyre J. W., Lorimer J. W., and Hill I. R. (1990) Detection of sulphur and polysulphides on electrochemically oxidized pyrite surfaces by X-ray photoelectron spectroscopy and Raman spectroscopy. *Journal of Electroanalytical Chemistry* **292**, 139-152.

Mysen B. and Frantz J. (1993) Structure of silicate melts at high-temperature - in-situ measurements in the system BaO-SiO2 to 1669°C. *American Mineralogist* **78**(7-8), 699-709.

Nachal'naya T. A., Andreyev V. D., and Gabrusenok E. V. (1994) Shift of the frequency and Stokes-anti-Stokes ratio of Raman spectra from diamond powders. *Diamond and related Materials* **3**, 1325-1328.

Nakamoto K. (1986) *Infrared and Raman spectra of inorganic and coordination compounds.* John Wiley and Sons.

Palmer D., Hemley R., and Prewitt C. (1994) Raman-spectroscopic study of high-pressure phase-transitions in cristobalite. *Physics and Chemistry of Minerals* **21**(8,), 481-488.

Pan P. and Wood S. A. (1991) Gold-chloride complexes in very acidic aqueous solutions at temperatures 25-300°C: A laser Raman spectroscopic study. *Geochimica et Cosmochimica Acta* **55**, 2365-2371.

Pasteris J. D. and Wopenka B. (1991) Raman spectra of graphite as indicators of degree of metamorphism. *Can.Min.* **29**, 1-9.

Pasteris J. D., Wopenka B., and Seitz J. C. (1988) Practical aspects of Quantitative Laser Raman Microprobe Spectroscopy for the Study of Fluid Inclusions. *Geochim.Cosmochim.Acta* **52**, 979-988.

Peck J. A., Tait C.D., Swanson B. I., and Brown G. E. J. (1991) Speciation of aqueous gold(III) chloride from ultraviolet/visible absorption and Raman/resonance Raman spectroscopies. *Geochimica et Cosmochimica Acta* **55**, 671-676.

Pironon, J. (1993) Estimation de la longeur de chaine des hydrocarbures des inclusions fluides par spectrometrie Raman *C.R.Acad. Sci. Paris II* **316,** 1075-1082

Raman C.V. and Krishnan K.S. (1928) A new type of secondary radiation *Nature*, **121**, 501

Renders P. J. and Seward T. M. (1989) The adsorption of thio gold (I) complexes by amorphous As_2S_3 and Sb2S3 at 25 and 90°C. *Geochimica et Cosmochimica Acta* **53**, 255-267.

Roberts S. and Beattie I. (1995) Micro-Raman Spectroscopy in the Earth Sciences. In *Microanalytical techniques in the Earth Sciences,* (ed. P. J. Potts, J. F. W. Bowles, S. J. B. Reed, and M. R. Cave), pp. 387-408. Chapman and Hall.

Roberts S. and Murray J. (1995) Characterization of cement mineralogy in agglutinated foraminifera (protista) by Raman-spectroscopy. *Journal of the Geological Society* **152**(pt1), 7-9.

Roberts S., Tricker P., and Marshall J. (1995) Raman-spectroscopy of chitinozoans as a maturation indicator. *Organic Geochemistry* **23**(3), 223-228.

Rosasco G. J., Roedder E., and Simmons J. H. (1975) Laser-excited Raman spectroscopy for non-destructive partial analysis of individual phases in fluid inclusions in minerals. *Science* **190**, 557-560.

Seitz J. C. and Pasteris J. D. (1990) Theoretical and Practical Aspects of Differential Partitioning of Gases by Clathrate Hydrates in Fluid Inclusions. *Geochim.Cosmochim.Acta* **54**, 631-639.

Seitz J. C., Pasteris J. D., and Chou I.-M. (1993) Raman spectroscopic characterization of gas mixtures. I. Quantitative composition and pressure determinations of CH4, N2, and their mixtures. *Am. Journ. Sci.* **293**, 297-321.

Seitz J. C., Pasteris J. D., and Wopenka B. (1987) Characterisation of CO2-CH4-H2O Fluid Inclusions by Microthermometry and Laser Raman Microprobe Spectroscopy: Inferences for Clathrate and Fluid Equilibria. *Geochim.Cosmochim.Acta* **51**, 1651-1664.

Seward T. M. (1991) The Hydrothermal Geochemistry of Gold., In Gold Metallogeny and Exploration (ed. Foster R. P.) Blackie

Shenberger D. M. and Barnes H. L. (1989) Solubility of gold in aqueous sulfide solutions from 150-350°C. *Geochimica et Cosmochimica Acta* **53**, 269-278.

Shikazono N. and Shimizu M. (1987) The Ag/Au ratio of native gold and electrum and the geochemical environment of gold vein deposits in Japan. *Mineralium Deposita* **22**, 309-314.

Tossell J. A. (1996) The speciation of gold in aqueous solution: A theoretical study. *Geochimica et Cosmochimica Acta* **60**, 17-29.

Vlassopoulos D. and Wood S. A. (1990) Gold speciation in natural waters: I. Solubility and hydrolysis reactions of gold in aqueous solution. *Geochimica et Cosmochimica Acta* **54**, 3-12.

Wang A., Jolliff B., and Haskin L. (1995) Raman-spectroscopy as a method for mineral identification on lunar robotic exploration missions. *Journal of Geophysical Research-Planets* **100**(E10,), 21189-21199.

White W. B. (1975) Structural Interpretation of Lunar andTerrestrial minerals by Raman Spectroscopy. In *Infrared and Raman Spectroscopy of Lunar and Terrestrial Minerals* (ed. C. J. Karr), pp. 325-359. Academic Press.

Wopenka B. and Pasteris J. D. (1986) Limitations to quantitative analysis of fluid inclusions in geological samples by laser Raman microprobe spectroscopy. *Appl. Spectrosc.* **40**, 144-151.

_____oOo_____